NOVA SCHOOL OF SCIENCE & TECHNOLOGY

DEPARTMENT OF MECHANICAL AND INDUSTRIAL ENGINEERING

ANTÓNIO CARLOS DOS SANTOS GUERREIRO

BSc in Mechanical Engineering Sciences

DEVELOPMENT OF A PROCESS TO MEASURE THE EXIT FLOW AREA OF THE LOW PRESSURE TURBINE NOZZLE FROM THE CFM56-5B ENGINE

MASTER IN MECHANICAL ENGINEERING

NOVA University Lisbon
november, 2022

NOVA SCHOOL OF
SCIENCE & TECHNOLOGY

DEPARTMENT OF
MECHANICAL AND INDUSTRIAL ENGINEERING

DEVELOPMENT OF A PROCESS TO MEASURE THE EXIT FLOW AREA OF THE LOW PRESSURE TURBINE NOZZLE FROM THE CFM56-5B ENGINE

ANTÓNIO CARLOS DOS SANTOS GUERREIRO

BSc in Mechanical Engineering Sciences

Adviser: João Fradinho
Assistant Professor, NOVA University Lisbon

MASTER IN MECHANICAL ENGINEERING

NOVA University Lisbon
november, 2022

Development of a Process to Measure the Exit Flow Area of the Low Pressure Turbine Nozzle from the CFM56-5B Engine

This document was created with the (pdf/Xe/Lua)LaTeX processor and the NOVAthesis template (v6.9.4) [1].

Acknowledgements

This dissertation is the culmination of a long and important journey on a personal and academic level. It would not be possible to conclude my master's without the support of the people mentioned below.

First of all, I would like to thank the TAP Engine Shop staff for the trust and availability offered that was crucial for the realization of this project. A big thank you to Engineer Sara Lucas and Engineer António Ferreira for receiving me so well and always being available to help. Thanks to all the TMA's, Reis, André, António and João for sharing all the knowledge that was essential to the realization of this project.

Thanks to all the members of *Departamento de Engenharia Mecânica e Industrial* in general that contributed to my development as a student and a human. A special thanks to Professor João Fradinho for his support and confidence in my abilities to car ry out this project. Thanks to professor António Mourão and Professor Rui Martins who contributed to memorably marking my academic career.

A big thank you to my coursemates "Alentejanos" who made this journey easier.

A warm thanks to my girlfriend, Leonor, for all the support she gave me during this period. And finally, the most important thanks to my mother, father, and sister, whom I love so much, for helping me to achieve all my personal goals.

And, at last but not least, a special thanks to engineer Mário Almeida Santos for all the kindness and support that was possible to give. It was a pleasure to have met you.

"Wisdom is the daughter of experience." (Leonardo da Vinci)

Abstract

Turbofan engine maintenance is an area that involves various technologies and advanced processes linked to the inspection and repair of engine components.

In TAP M&E's Engine Shop, several repair processes are used to ensure each engine part's total reconditioning. In the dimensional inspection section, high-precision measuring methods are required in order to verify the parameters required by the manufacturer. The measurement of the low pressure turbine nozzles' exit flow area from the CFM56-5B engine is an undeveloped dimensional inspection process in TAP Engine Shop. However, advances in this field could represent a considerable efficiency increase regarding the inspection processes.

Knowing that the values of these areas influence the engine capacity, it is crucial to create an accurate measurement method that allows these values to be compared with the reactor performance obtained on the test cell. With the equipment available in the Engine Shop - HandyScan 3D and Mitutoyo Euro-C 121210 - the objective of this study is to create a program in CMM that will perform automated measurements of the exit flow areas. This study could be introduced as a task that is part of the production level inspection of these components.

Keywords: Dimensional Inspection, Turbofan Engine, Nozzle, Exit Flow Area, Coordinate Measuring Machine, Fixturing Tool.

Resumo

A manutenção de motores *turbofan* é uma área que envolve várias tecnologias e processos avançados ligados à inspeção e reparação de componentes de motores.

Na oficina de motores da TAP M&E, são utilizados vários processos de reparação para assegurar o recondicionamento total de cada peça do motor. Na área da inspeção dimensional, são necessários métodos de medição de alta precisão a fim de verificar os requisitos exigidos pelo fabricante. A medição da área de escoamento à saída das *nozzles* das turbinas de baixa pressão do motor CFM56-5B é um processo de inspecção dimensional que não se encontra desenvolvido na oficina de motores da TAP. No entanto, os avanços neste campo poderiam representar um aumento considerável da eficiência no que diz respeito aos processos de inspeção.

Sabendo que os valores destas áreas influenciam a performance do motor, é crucial criar um método de medição preciso que permita a comparação destes valores com o desempenho do motor obtido no banco de ensaio. Com o equipamento disponível na oficina de motores - HandyScan 3D e Mitutoyo Euro-C 121210 - o objectivo deste estudo é criar um programa em CMM que irá realizar medições automatizadas das áreas de escoamento à saída. Este estudo apresenta potencial para ser introduzido como um processo que faz parte da inspecção destes componentes.

Palavras-chave: Inspeção Dimensional, Motor *turbofan*, *Nozzle*, Área de escoamento à saída, Máquina de Medição de Coordenadas, Ferramenta de fixação.

Contents

List of Figures

List of Tables

Acronyms

AM Additive Manufacturing 32, 47, 48, 58

BPR Bypass Ratio 5, 6, 8

CMM Coordinate Measure Machine 2, 3, 18, 20, 21, 29, 31, 33, 50, 51, 58
CNC Computer Numerical Control 33, 41, 50

DoF Degrees of Freedom 18, 19, 32, 39–43
DP Design Parameters 31

EGT Exhaust Gas Temperature ix, 13

FR Functional Requirements 31, 32, 34

HPC High Pressure Compressor 6, 8–10
HPT High Pressure Turbine 6, 9, 10, 12, 27

LPC Low Pressure Compressor 6, 8
LPT Low Pressure Turbine 1, 2, 6, 9, 10, 12, 17, 21, 22, 27, 32, 33, 52, 55, 67, 68

ME Maintenance and Engineering 1, 3

NGV Nozzle Guide Vanes 12, 14, 22

RPS Reference Point System 61

TAP Transportes Aéreos Portugueses 1–4, 16, 31, 34, 51, 66
TMA *Técnico de Manutenção Aeronáutica* 29, 34, 50, 58, 66

1 Introduction

Aviation has come a long way since the early days. Despite the fallout of the last pandemic years, the aircraft industry has become one of the most effective means of transport. International aviation is responsible for a considerable percentage of carbon dioxide emissions that are partly responsible for climate change. With this inflow, the aeronautical sector has a vital role in the environmental subject. If the aviation industry wants to follow the same growth path as it has in the past, it will need to reduce its environmental impact, or it may otherwise face regulatory restrictions.

This impact has become an increasingly powerful influence on aircraft design to reduce fuel consumption and develop airplanes into a more sustainable way of traveling. Several of the airplane's components are evaluated to make this transport more efficient with all the present technology in commercial aircraft. An aircraft's engine is directly related to fuel consumption and is, therefore, the component of the aircraft that can improve the most in this area.

The engine shop at Transportes Aéreos Portugueses (TAP) Maintenance and Engineering (ME) is responsible for maintaining airplanes' engines and is in constant progression as global air transport does not stop expanding. Part of this progress is the continual improvement of the processes used for the inspection and repair of aircraft engine components. This thesis will focus on developing a measuring strategy to dimensionally inspect the exit flow areas of the first stage Low Pressure Turbine (LPT) nozzles from the CFM56-5B, the engine that equips one of the world's best-selling airplanes of all time - Airbus A320.

1.1 Motivation

The aeronautical industry is one of the areas where it is most evident that engineering plays a fundamental role in technological and economic progress. There are multiple engineering areas (such as materials engineering, electrical engineering, aerospace engineering, mechanical engineering, and others) that perform critical duties in various airplane components.

Aircraft maintenance and, in this case, the maintenance of an airplane engine is an industry of great responsibility since a mechanical failure in the engine compromises the safety of hundreds of people in case of an accident. It is an area with no room for half-certainty, where the slightest failure can lead to a catastrophe.

This responsibility means that rigorous and precise work is required on the engineering side always to guarantee the correct operation of the engine. This area needs a broad knowledge and profoundness of virtually all fundamental engineering principles. In engine maintenance, several procedures of interest to mechanical engineering are used, such as repair and inspection processes, engine disassembly and assembly, and performance tests on the test cell, among others.

1.2 Objectives

Several engine components can influence the performance requirements of an engine, and the LPT nozzles have a crucial role in this matter. This component is submitted to high stresses and thermal impacts due to its location in the engine core. LPT nozzles dimensional inspection of exit flow areas is not performed at TAP at the moment, despite the decisive impact that this parameter has in engine efficiency.

Using the equipment available in TAP Engine Shop, the 3D scanner and the Coordinate Measure Machine (CMM), it is relevant to design an effective process of measuring exit flow areas. This process will permit to relate those areas with engine performance tested in the test cell. This thesis aims to develop a program to run automatically to dimensionally inspect the exit flow areas of the LPT nozzle. This study is the beginning of a vast project that TAP is interested in introducing in the Engine Shop.

1.3 Contents

This document is divided into seven chapters. The current chapter provides an introduction to the themes addressed to this thesis and explains its motivation and objectives.

The second chapter has a resumed description of the company, focusing on the engine's maintenance and engineering department. This chapter also contains a summary of the company's services and a description of the turbofan engine - CFM56-5B. A brief description of the engine's major modules, their components, and their operation is included with the engine representation to offer a better understanding of some of the subjects that may be covered in subsequent chapters.

The third chapter involves the LPT nozzles geometry and their impact on engine efficiency and capacity. It is described the fundamental geometric parameters that will be addressed in other chapters. Reviews some literature, namely some articles published by Rolls-Royce where is covered the influence that exit flow areas have in terms of capacity and demonstrated the importance of inspecting these components dimensionally.

The inspection done at the moment in TAP ME engine shop and the plan to develop a measurement process in CMM is covered in the fourth chapter. In this chapter is also resumed the available equipment and a brief description of the technical and capacity of each equipment - Creaform Handyscan 3D and Mitutoyo Euro-C 121210 - necessary to develop the inspection process.

The fifth chapter discusses the method to obtain a mesh model of the nozzle using Creaform Handyscan 3D and the construction steps of a parametric CAD model in SolidWorks. The accuracy of the CAD model comparing to the mesh model is a crucial parameter to guarantee the potential of the CMM program.

A fixture tool is necessary to guarantee: condition of immobility in a kinematic analysis, reduced inspect operation time and location accuracy. The sixth chapter addresses the fixture's design based on Axiomatic Design Theory. The calculation of the external forces and the fastening system are also important topics discussed in this chapter.

The seventh chapter is the culmination of dimensional inspection done in CMM. The location of the exit flow area is covered in this chapter as well as the entire development of the CMM program to obtain area values. In order to overcome adversities that occurred, unique methods were used such as:

- Localized mesh treatment to reduce the file size to create capacity to be processed by SolidWorks;
- Artifact creation in the CAD model so is possible to select a cutting plane in MCOSMOS to define the exit flow area section;
- Creation of reference planes in the CMM program to project the area contour to be possible the direct calculation in MCOSMOS.

The eighth and final chapter concludes the work done and highlights some of its accomplishments in connection to the larger project for correlation research. This chapter also discusses some of the future work that may be done to complete and provide other students the work of this thesis, as well as some acknowledgement of areas for additional development.

2

Company and CFM56-5B Engine

2.1 TAP Maintenance & Engineering

TAP Air Portugal Maintenance & Engineering Unit is located in Lisbon, Portugal, and is responsible for performing maintenance and engineering support to services such as Aircraft Maintenance, Engine Repair and Overhaul, Components Repair and Overhaul, Continuing Airworthiness Management, Engineering Services, Technical Laboratories, and Training [2].

TAP M&E has a workplace policy of Care2Quality that has as main pillars Safety, Quality, and Relationship and can be divided into all of his products and services [2]:

- Care2Airframe
- Care2Engines
- Care2Components
- Care2Engineering
- Care2TechnicalLabs

Each service is dedicated to its specific area and leads to Engine Shop having more than 50 years of operation with international recognition for its quality and reliability.

TAP M&E provides a comprehensive range of MRO (Maintenance, Repair, and Overhaul) services to commercial aircraft operated by TAP and third-party companies. TAP M&E, as part of the TAP group, provides the benefits of a comprehensive range of integrated services.

2.2 Turbofan Engine

Two main basic mechanisms of gas turbine engines can be used for aircraft propulsion: turboprop and turbojet engines. Turboprop engines use the exhaust flow of air to operate

a propeller that produces thrust, whereas turbojet engines use combusted airflow from the exhaust to generate thrust.

These two different mechanisms present limitations and are efficient under various operating conditions. The limiting factor for turboprop engines is related to the propeller speed generated by the airflow. Propeller loses their thrust production when their blade reaches supersonic speeds [3]. Turbojet engines have higher efficiency as the airspeed increases, and this means that for low rates, turboprop engines have higher efficiency than turbojet engines.

These characteristics have led to combining these two types of engines on the most common engine these days: the turbofan engine. A turbofan uses technology from both mechanisms to produce an engine that deals with more significant air flows and lower jet velocities compared with the turbojet, although higher propulsive efficiency compared with the turboprop engine.

Turbofan is the standard engine for commercial aircraft propulsion due to its high fuel efficiency. This engine is an evolution from the pure turbojet engine and the turboprop engine. In a turboprop engine, most of the airflow bypasses the engine core. All the air taken passes through the core engine in a turbojet engine. This leads to the concept of Bypass Ratio (BPR) [3].

The BPR is the relation between the mass of air bypassing the engine core (bypass airflow) and the mass of air going through the core (core airflow), which is illustrated in Figure 2.1. Considering $\dot{m}_1$ core mass airflow and $\dot{m}_2$ bypass mass airflow, BPR is defined by:

$$BPR = \frac{\dot{m}_2}{\dot{m}_1} \tag{2.1}$$

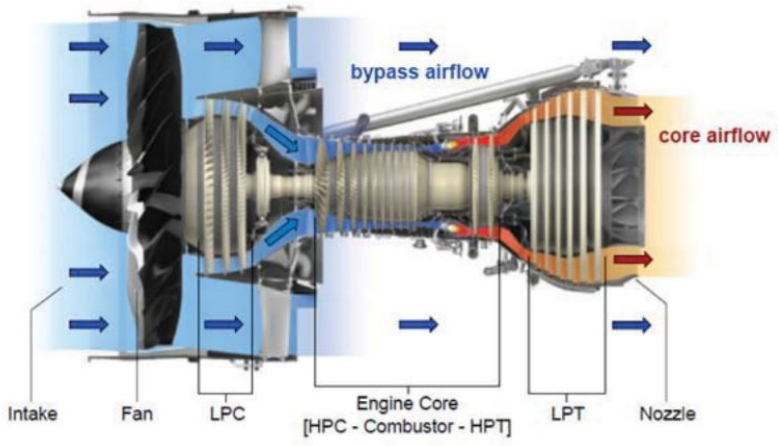

Figure 2.1: Turbofan Engine. [3]

Low BPR turbofan engines are mostly used for military purposes and are equipped with an afterburner, alternately high BPR engines are most common in commercial airplanes. Commercial aircraft turbofan engines produce thrust from a combination of both

air flows with a BPR of around 5. The working cycle for this type of engine, according to [3] can be resumed in four stages that occur simultaneously:

- **Compression**
  - During compression, the intake air pass through a fan and is divided. The core airflow is compressed and preheated by first the Low Pressure Compressor (LPC), or Booster, and then the pressure increases even more when it enters the High Pressure Compressor (HPC). Bypass airflow is driven to the fan duct.
- **Combustion**
  - In this stage, accelerated core airflow from the HPC enters into the combustion chamber where is injected fuel and it occurs the combustion. The thermal energy increases while the pressure stays constant. This results in an increase of the potential energy.
- **Expanding**
  - The burned air and fuel mixture stream enters the High Pressure Turbine (HPT) and then the LPT. The core airflow is expanded and the potential energy associated with the high temperature and high pressure is converted to kinetic energy. This kinetic energy is translated to a rotation movement of the shaft that is connected to the fan and the compressor module.
- **Exhaust**
  - In this final stage, the core airflow is mixed with the bypass airflow, well represented in Figure 2.3. Both are responsible for generate thrust.

These four stages are represented in Figure 2.2.

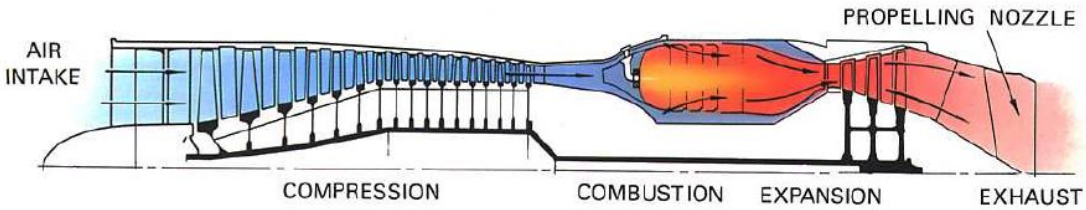

Figure 2.2: Working cycle of a Turbine Engine. [3]

Most of the turbofan engines are equipped with a two spool configuration, that is schematized in Figure 2.3. This disposition permits to have two concentric shafts rotating at different speeds. This means that is possible to have low angular velocity, N1 speed, for the LPC and LPT in relation with the HPC and HPT, N2 speed. HPC and HPT are represented in black in Figure 2.3. As the low pressure components has larger diameter

this configuration permits the engine to operate at high speeds without compromise the tip velocity to transcend the subsonic speed.

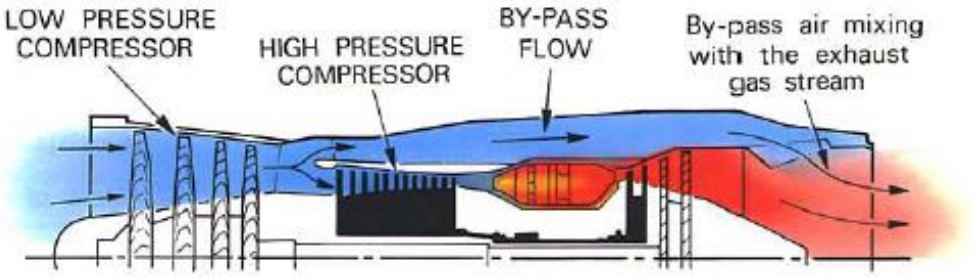

Figure 2.3: Two spool configuration. [3]

2.3 CFM56-5B Engine

2.3.1 CFM56 Family

CFM International is a joint company formed by equal parts of General Electrics and SNECMA. They took advantage of a unique market opportunity to develop a complete modern turbofan engine. It started with the CFM56-2 but rapidly expanded to develop two derivative versions of this product: the CFM56-3 designed specially for the Boeing 737 series and the CFM56-5 for the Airbus A320 and A340 series.[4]

The CFM56 engine family is represented in Figure 2.4, according to their thrust force and aircraft's applications, based in CFM manual.[5]

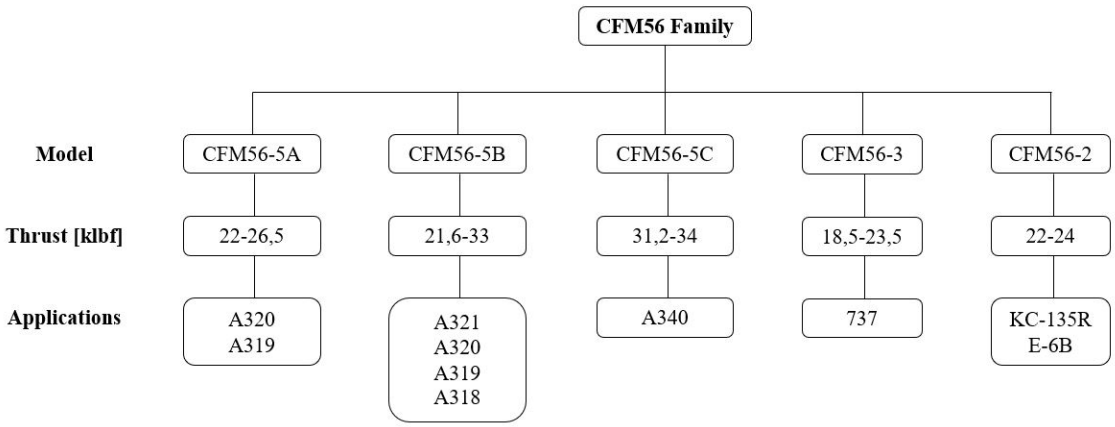

Figure 2.4: CFM56 Family.

The CFM56 engine was the first to receive certification from the Federal Aviation Agency and *Direction Generale de L'Aviation Civile*. This certification permits providing clients with parts data, information, and technical guidance to ensure that the agencies' regulations and requirements will maintain the engine.

2.3.2 CFM56-5B

CFM56-5B is an high BPR engine with two spool axial flow that equips Airbus models like A319, A320 and A321. It is supported by the wing pylon and streamlined by cowlings. All this section is based in information present in engine manual [6]. In Table 2.1 are represented a few engine characteristics.

Table 2.1: CFM56-5B general characteristics.

Characteristic	Value
Length [m]	2,94
Height [m]	2,14
Width [m]	1,97
Weight [kg]	2381
Thrust [klbs]	22 to 33

The CFM56-5B is a modular concept design engine, and it can be divided in three distinct major modules and one accessory drive module that are represented in Figure 2.5.

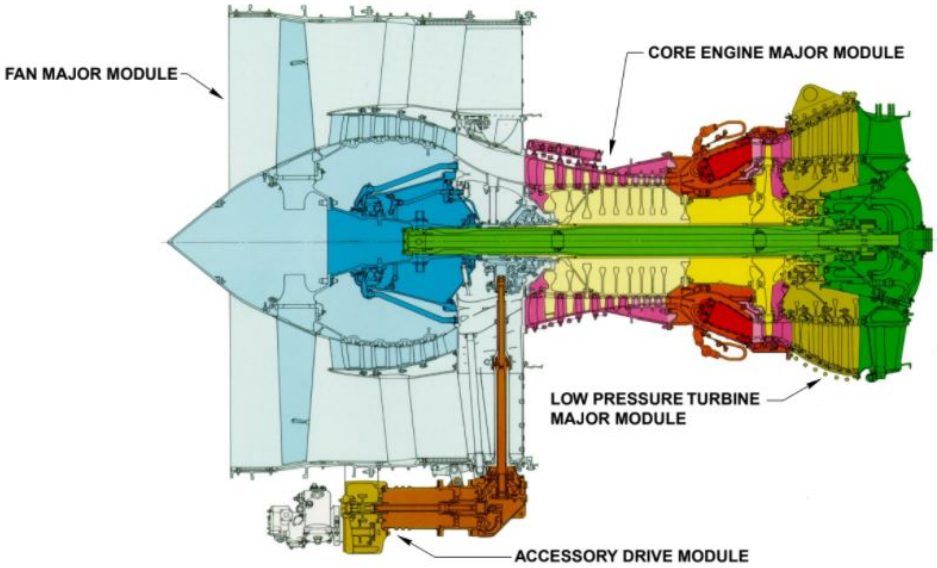

Figure 2.5: CFM56-5B Modules. [6]

General Electrics is responsible for developing the Core Engine Major Module, and SNECMA is responsible for developing the outsider modules.

2.3.2.1 Fan Major Module

The Fan Major Module, represented in Figure 2.6, is constituted by a fan and LPC that is also called booster. Those components have an angular velocity N1 as they are connected to the low pressure spool. This module is responsible to accelerate air overboard to generate thrust and to increase the pressure of the air that enters the HPC.

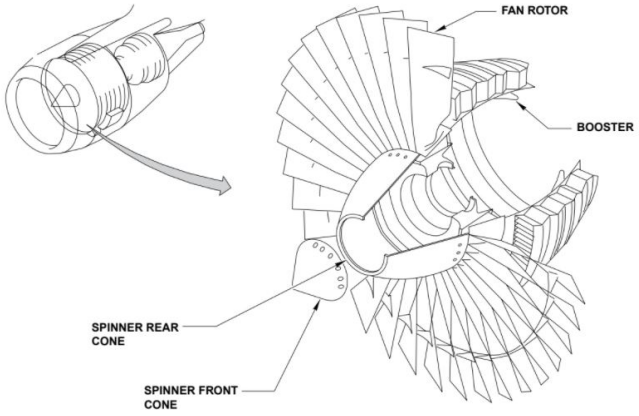

Figure 2.6: Fan Major Module. [6]

2.3.2.2 Core Engine Major Module

The Core Engine Major Module is responsible to increase the pressure and thermal energy of the core airflow. It embodies the HPC, the combustion sector, the HPT and the first stage of LPT nozzle. The rotors of HPC and HPT belong to the high pressure spool, so have the same angular velocity, N2. This module is responsible to produce the power to generate thrust and is represented in Figure 2.7

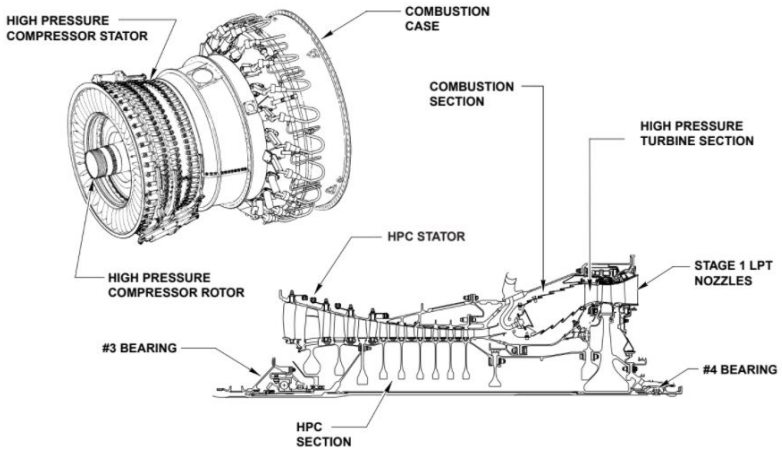

Figure 2.7: Core Engine Module. [6]

Between the combustion chamber and the first stage of rotor blades from HPT, exists one stage of stator nozzle vanes or the HPT nozzles that accelerates and directs the burnt airflow to incite HPT rotor blades with certain velocity and direction.

HPT Nozzles are positioned next to the combustion chamber and LPT nozzles are positioned next to the HPT blades. These components are submitted to huge thermal impact as the airflow leaves the combustion at high temperatures. For this reason the cooling system of these components are crucial for the safe and efficient operation of the engine.

Air from the fourth and fifth stage of the HPC is deviated and ducted, through four

pipes, to cavities of the HPT Nozzles and LPT Nozzles with the intention to lower the temperature while the engine is running. To cool down HPT rotor, the air is ducted through two pipes from the fourth and ninth stages of HPC.

In this module, as to disassemble for inspection is not practical, there are borescope ports, so it facilitates the interior inspection. These ports are located in fixed positions and are numbered with the letter S in first. In Figure 2.8 there is an example of the location of borescope ports in the combustion case.

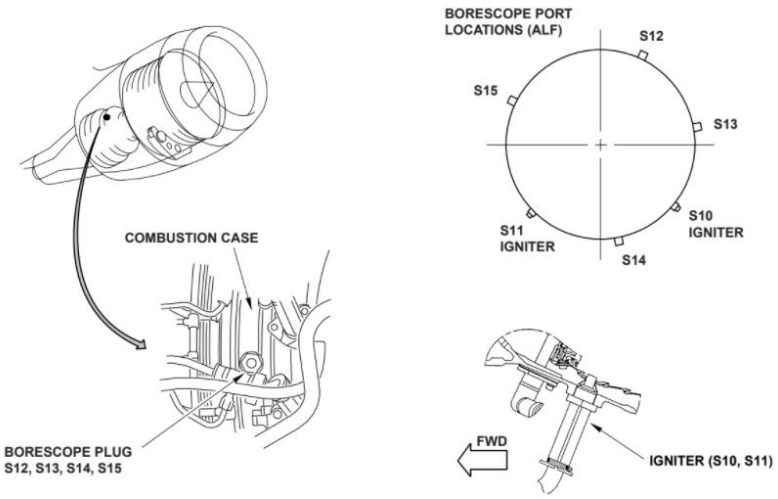

Figure 2.8: Borescope ports locations in the combustion section. [6]

2.3.2.3 Low Pressure Turbine Major Module

The LPT module is constituted by four stages and converts the rest of energy from HPT of combustion gasses into the necessary torque to drive the fan and booster rotor. LPT rotors are connected to the same shaft, the low pressure spool, of fan and booster rotor. In other words, have the same angular velocity N1.

Low Pressure Turbine Module is represented in Figure 2.9.

2.3.2.4 Accessory Drive Section

In order to drive the engine accessories, part of the core engine power is extracted through the Inlet Gearbox. The accessory drive system transmits external power from the engine air starter to drive the engine.

In CFM56-5B model engine Radial Draft Shaft is connected to the high pressure spool with velocity N2. Accessory Gearbox permits reduce or increase the velocity to drive the following accessories:

- Lube Unit;
- Hydraulic Pump;

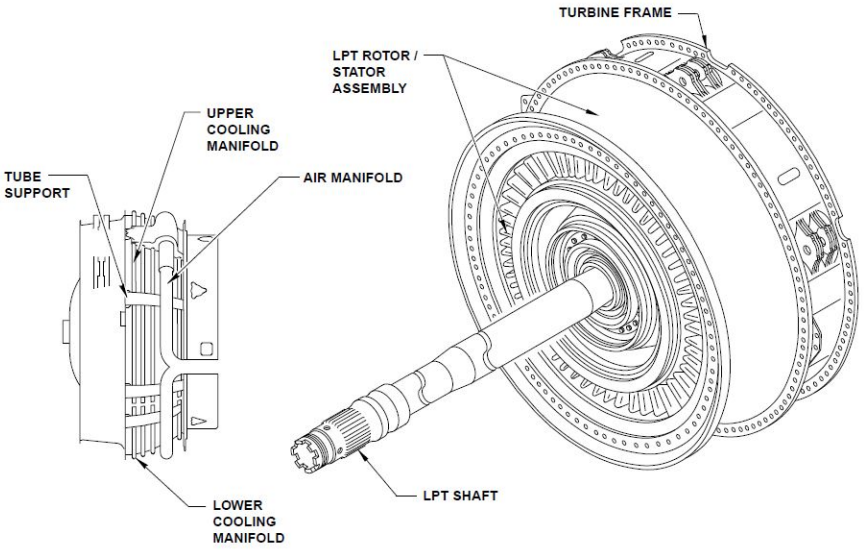

Figure 2.9: Low Pressure Turbine Module. [6]

- Hand-cranking Drive;
- Control Alternator;
- Integrated Drive Generator;
- The Fuel Pump;
- The Starter;

In Figure 2.10 is represented the Accessory Drive Section.

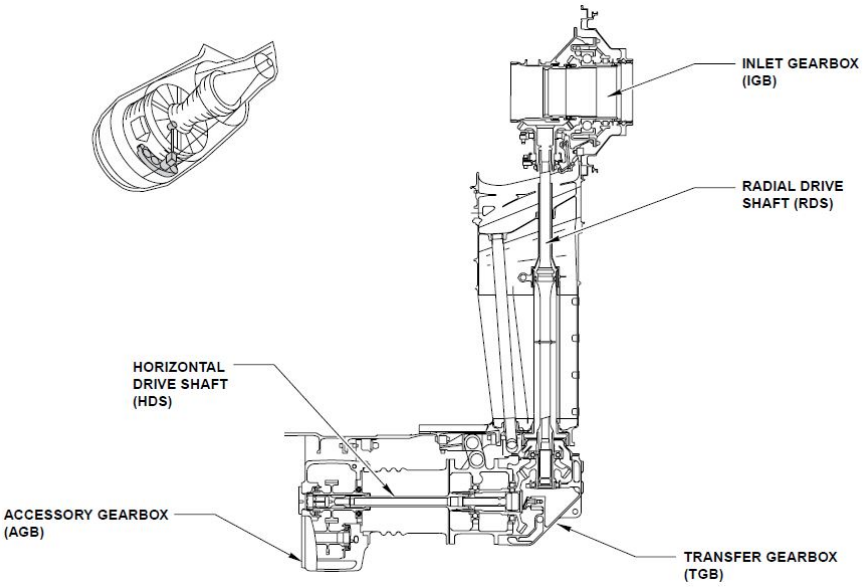

Figure 2.10: Accessory Drive Section. [6]

3

LPT Nozzles Geometry and Impact on Engine Efficiency

Stage one LPT nozzles are one type of Nozzle Guide Vanes (NGV) from Core Engine Major Module, that can be seen in Figure 2.7. These nozzles can influence the entire engine behavior since these vanes are located between the HPT and LPT rotor blades, where the airflow has considerable values of pressure and temperature to transform into kinetic energy. In Figure 3.1 is possible to visualize their shape and how they are fixed. These illustrated nozzles are merely representative, the workpiece in study do not have this exact geometry configuration.

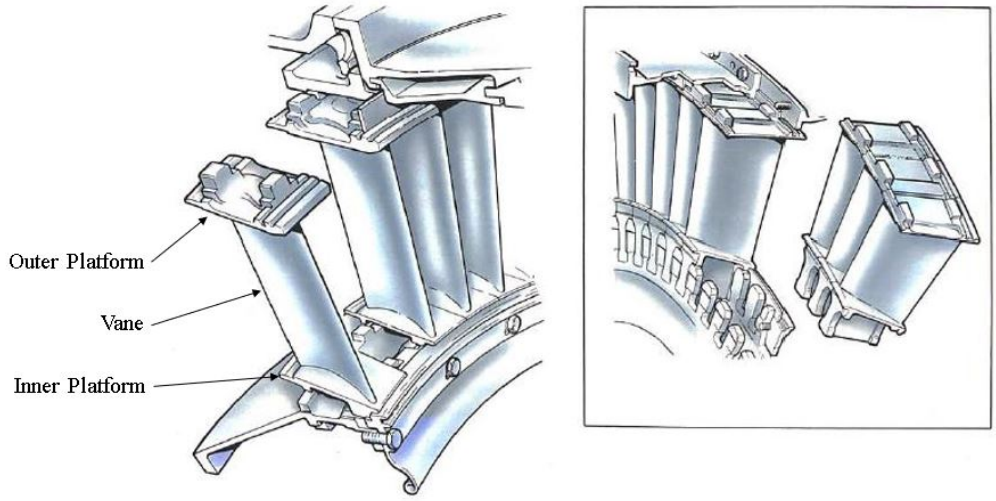

Figure 3.1: NGV's shape and fixture, adapted from Rolls-Royce study [3].

NGV's vanes have an airfoil shape and are responsible for accelerate and direct the gases coming to the turbine rotor blades. Figure 3.2 is an example of the flow path and the effect of NGV's. To be noticed that the nozzle vanes have a stationary position in relation to the turbine rotor blades that present a rotational movement.

Because of their stationary position, the stresses associated with rotation are residual when compared to the turbine rotor blades. Due to their location, heat resistance is the

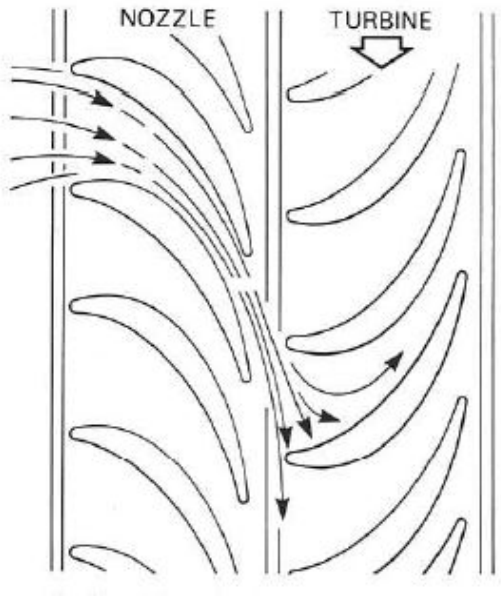

Figure 3.2: NGV's flow path [3].

most crucial property when it comes to material evaluating. High temperature resistance nickel alloys are used with ceramic coating in this type of pieces, since the Core Engine Module achieves high temperature values in operation. The material capacity to deal with high temperatures is essential to minimize the cooling flow because the lower the cooling requirement for components, the greater the engine efficiency. [7].

3.1 Deterioration of Turbine Nozzles

As engine operation time increases, performance starts to decrease due to deterioration phenomenons. The losses can be related with theEGT, in Figure 3.3 is represented a typical high bypass engine deterioration in terms of hours of operation [7].

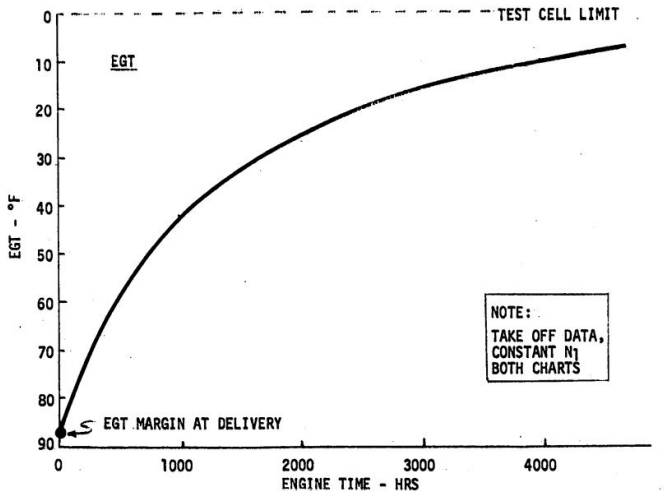

Figure 3.3: EGT in order to hours of operation on a typical high bypass engine [7].

The deterioration of a turbine engine can be divided into short-term and long-term deterioration. When the engine is brand new, all the engine components have tight tolerances, and the performance is how it was designed. After 1000 hours of operation it occurs losses due to seal problems, and at 3000 hours of operation, it starts to occur changes in blade profiles caused by erosion. Long-term engine deterioration is most related to hot sections stresses, for example, in the HPT zone [7].

NGV's are submitted to a relevant thermal impact due to their location on the engine core. Thermal fatigue and severe erosion are two concerns when it comes the deterioration of NGV.

3.2 NGV Geometry

To study NGV geometry is relevant to understand the nomenclature of the geometric parameters.

The principal geometric parameters that matter for this study are all reunited in Figure 3.4.

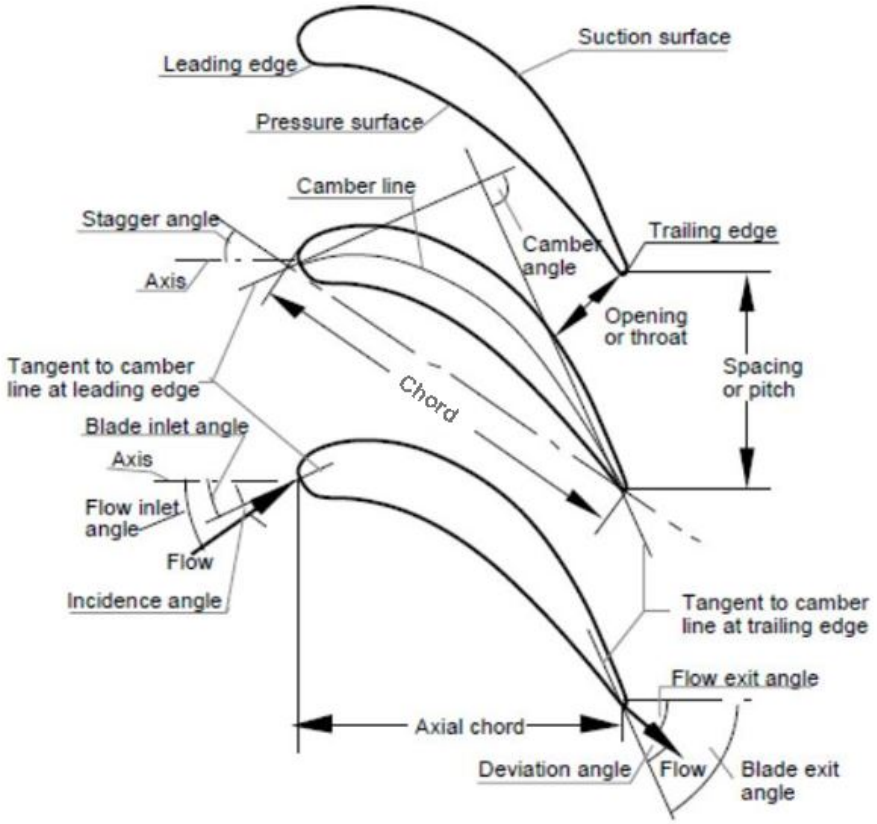

Figure 3.4: NGV's geometric parameters [8].

Exit flow area correspond, normally, to the area of the narrowest cross-section between the suction surface from one vane and the pressure surface from the next vane, which

is represented in Figure 3.4, as opening or throat. This area has a huge influence on the gas flow, since it is the section where the flow reaches maximum velocity. The plane that defines the exit flow area is defined by the lines represented in Figure 3.5, perpendicular to the plane of the paper. In this study, it was considered two distinct exit flow areas and was compared the results in terms of capacity when altering the geometric parameters.

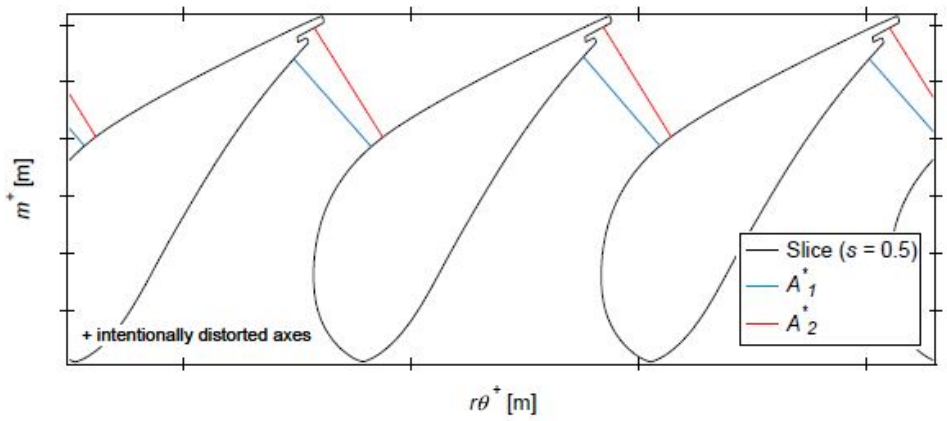

Figure 3.5: NGV's exit flow area [9].

Some vanes can present a torsional feature in their geometry where is associated a twisted angle, represented in Figure 3.6.

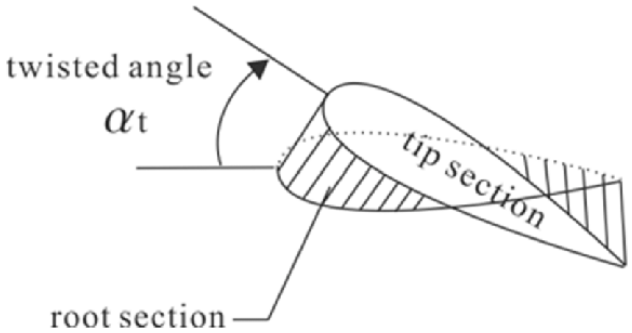

Figure 3.6: Twisted angle [10].

3.3 NGV's Geometry Impact on Engine Efficiency

The geometric shape of the vanes can influence the flow of the gases aerodynamically. It is known that the narrowest cross-section determines the passage in terms of velocity and direction. That said, it is vital to study and verify geometric variations and their effect on the engine's performance. [9]

Studies have been made [9] to analyze the capacity Γ of a turbine engine with parametric geometry variation. The capacity of a nozzle vane is defined by the equation:

$$\Gamma = \dot{m}\frac{\sqrt{T_t}}{p_t} \tag{3.1}$$

Wherein $\dot{m}$ represents the inlet mass flow, T_t is the total temperature and p_t the total pressure at inlet. The capacity is a good parameter to measure the engine efficiency. In this study [9], was concluded that the variation of the profile offset at suction side, P_{SS} and the trailing edge slot position, p_{TES} (variation represented in Figure 3.7(a)) influence significantly the capacity due to their effect on the effective narrowest cross-section. This influence is illustrated in Figure 3.7(b).

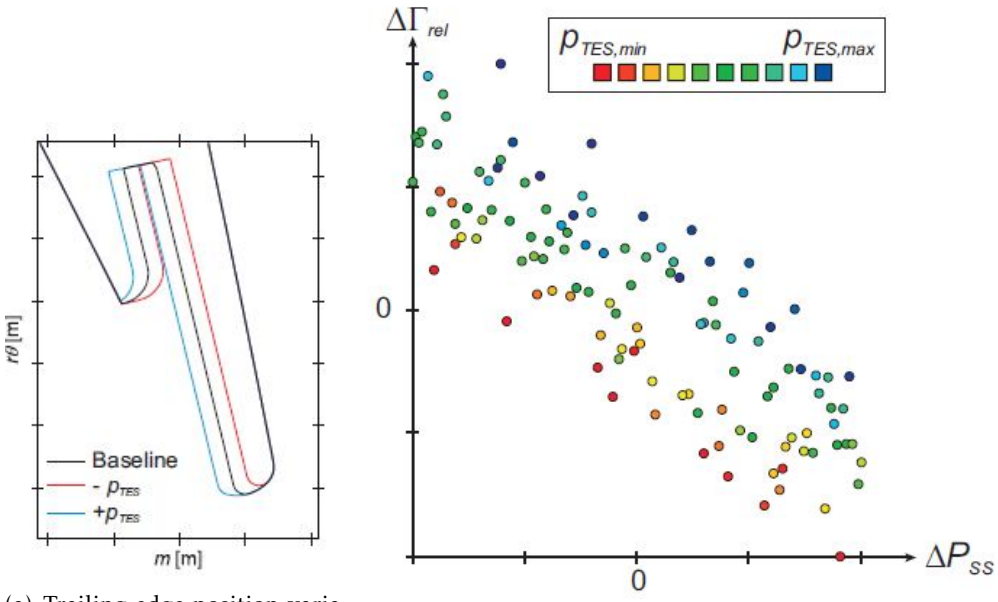

(a) Trailing edge position variation.

(b) Capacity variation in order to P_{SS} and p_{TES}.

Figure 3.7: Study of variation of capacity related to design parameters [9].

This study reflects the importance and TAP interest in proceeding with this project as it can be seen that the geometric parameter in studying can influence the overall engine performance.

4

TAP M&E Inspection

TAP M&E is always in progress to develop efficient methods to become more productive in maintenance and inspection operations. Thus, air companies' collaboration with universities allows students to progress in their inspection methods with the available equipment in the facility. For the realization of this thesis, the available equipment will permit obtaining a mesh of the LPT nozzle under study in order to create a CAD model of the workpiece and measure the exit flow areas using a CMM.

4.1 Available equipment

This process will be developed with the equipment available at TAP M&E's engine shop. Part of TAP interest is to maximize the capability of the machinery to obtain efficient methods of operation. Briefly, the following equipment used will be the Creaform Handyscan 3D, that will permit to obtain a mesh model of the workpiece and the Mitutoyo Euro-C 121210, where is going to be developed a program to measure exit flow areas.

4.1.1 Laser Scanner

Creaform HandySCAN 3D is a precise laser scanner that presents technical data that allow the creation of an accurate reference mesh model [11]:

- Accuracy: 0,025 mm
- Volumetric accuracy: 0,020 mm
- Measurement resolution: 0,025 mm
- Measurement rate: 1300000 measurements/s

The scanner works with a ranging sensor that calculates the distance between the sensor and a set of points on the surface. For each point are generated three-dimensional coordinates that settle in space. [12]

The software that works in parallel with the scanner is the *VXelements*. In this program is possible to control different parameters of the scan process, for example, it is possible to define the resolution, where the lower the value, the longer the processing time. Another important parameter is the shutter speed, which is defined by the duration of time that the scanner is open to allow light into the ranging sensor. Shutter speed has a massive influence during the recognition of low-light surfaces, during the scan is possible to oscillate the shutter value to optimize the achievement of points in dark zones. Figure 4.1 is possibly to see the Creaform HandySCAN 3D equipment.

Figure 4.1: Creaform's Handy Scan 3D.

This equipment is very easy to handle and makes scanning much accessible comparing to other scans. This mobility allows to constantly change the position of the scanner during operation, which greatly reduces the process time of obtaining a complete and closed mesh.

4.1.2 Coordinate Measure Machine

CMM is an equipment for measuring various parts and components' geometry using the sensing of a precise probe's mechanical touch. Different measuring methods are used by other types of CMM's beside this one, there are measuring systems that use lasers or optical tips, for example. The motions of the machine axes in the Mitutoyo Euro-C 121210 CMM are numerical computer controlled, normally, in a three-dimensional coordinate system.

This machine has movement in 5 Degrees of Freedom (DoF), i.e., apart from the linear movements in the three-dimensional directions, this CMM allows controlling two probe angles that permit the measurement of surfaces that would never be possible. The constitution of this machine is defined by: the granite bed, the probe, the probe tree, the arm, the joystick and the software, represented in Figure 4.2.

The five degrees of freedom are defined by the three translation degrees (X, Y, and Z) plus two rotational degrees of the probe (θ and β). In Figure 4.4 is represented the rotational angle θ around its Y axis. In Figure 4.5 is represented the rotational angle

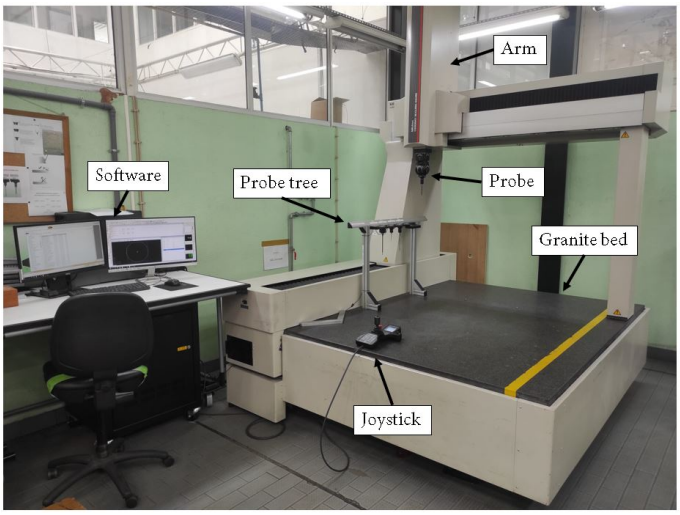

Figure 4.2: CMM constitution.

β around its Z axis. In Figure 4.3 is represented the X and Y axis, where the Z axis is perpendicular to the granite bed. Notice that the probe tree is represented in dark grey at the left of Figure 4.3.

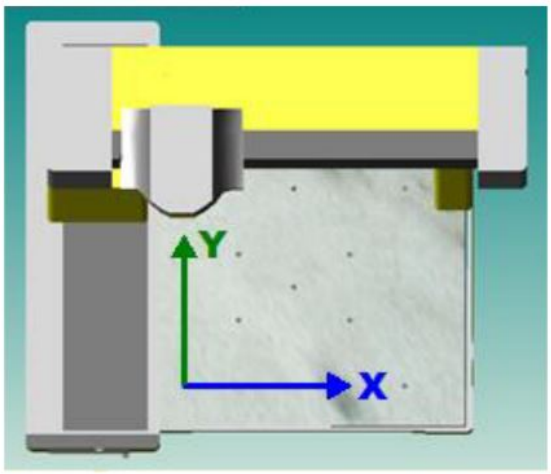

Figure 4.3: Top view of the CMM with the X and Y axis represented.

In probe tree, there are two probes available and capable to accomplish the intended inspect to be done: RSP2-3 and RSP-3. These probes present different characteristics that can be limiting depending on the geometry to be measured. In Table 4.1 are represented the specifications of RSPP2-3 and RSP3:

Table 4.1: Available probes characteristics.

Probe	DoF	Countor	Sphere
RSP2-3	5	2D	6 mm
RSP-3	3	3D	4 mm

The RSP3-2 probe has the ability to obtain three-dimensional contours, however, it

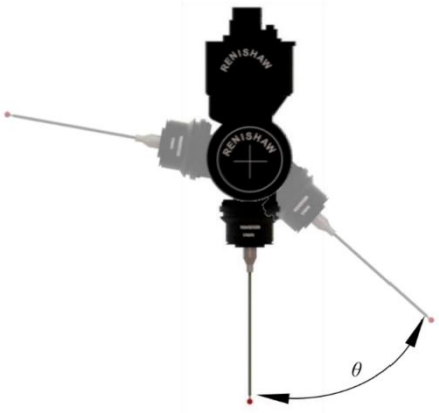

Figure 4.4: Rotational angle around its Y axis [13].

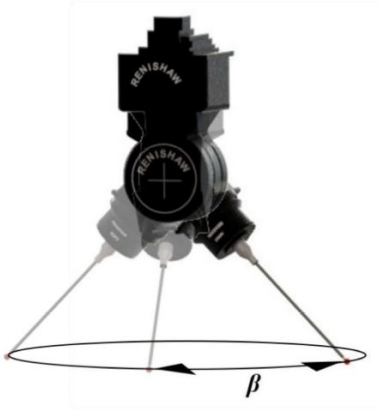

Figure 4.5: Rotational angle around its Z axis [13].

is limited to a measurement where the θ and β angles are fixed. Whereas with the RSP2 probe, there is the possibility for the probe to scan a profile while moving the angles associated with the probe. This movement allows a more fluid measurement that is often used for dimensional intersection of airfoil sections.

The work space of the CMM is an essential specification since the development of the program and the fixture must be in accordance to the available volume. This volume is represented in Figure 4.6, whose dimensions are 1200x1200x1000mm.

In terms of software that works in parallel with the CMM, this machine runs through Mitutoyo's MCOSMOS software program. This software is responsible to manage CMM functions and to give access to the GEOPAK module where the program is developed for part inspection and the STEP file is opened to allow virtual manipulation [14]. Furthermore, the software CAT1000PS is used to physically run the code from the GEOPAK into the CMM. A bridge, however, is required to transfer the produced software from the GEOPAK to the CAT1000PS. This bridge is made possible by a UCC Server, which receives and sends code in the I++ protocol [15]. The hierarchy of software packages is represented in Figure 4.7.

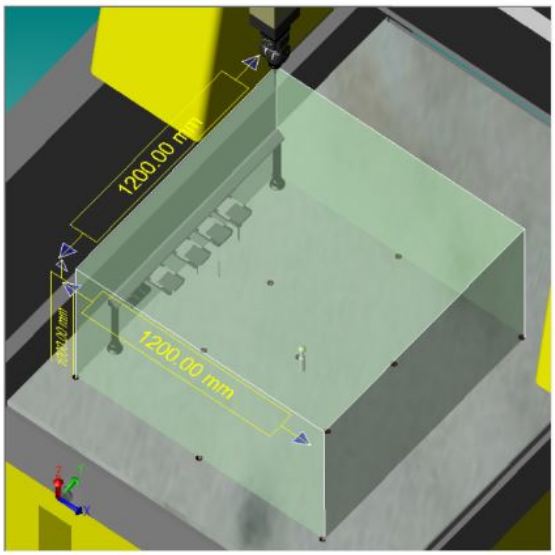

Figure 4.6: CMM Work volume.

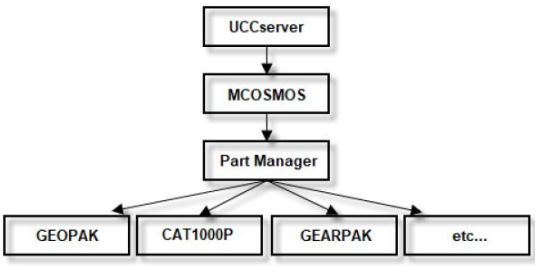

Figure 4.7: CMM hierarchy of software packages.

The GEOPAK module permits to develop a new part inspection program. In this section there is access to two measuring modes: Learn Mode and Repeat Mode. Parts can be manually measured in learn mode. The learn mode feature is also used to "teach"the CMM how to measure a part in the context of programming automatically.

The Repeat Mode function allows the automatic measurement of parts by selecting the existing program (created in Learn Mode, for example) for the part you want to inspect. Part of the objective of this thesis is to develop the program to measure exit flow areas of LPT nozzles.

Mitutoyo's CAT1000P has great potential to TAP M&E to develop dimensional inspection in CMM. This module has the benefit to create programs with minimum manual data input. Allows generating and simulating the probe's route for a set of measurements. To minimize contact with the model, this movement simulation allows the generation of the whole measurement program through a virtual 3D representation.

4.2 TAP M&E Past Work

Universities have been in contact with TAP M&E. One of the recent researches was the master thesis by Farinha, E. [16] that studied a fixture design and developed a method of measuring the HPC rotor blades (achievements represented in Figure 4.8). This study is a continuation of the master thesis by Rendas P. [13] that started the development of the fixture of the HPC rotor blades. Also, a master thesis by Baptista F. [17] contributed to this work by studying a model that predicts the off-design performance of the CFM56-5B turbofan engine.

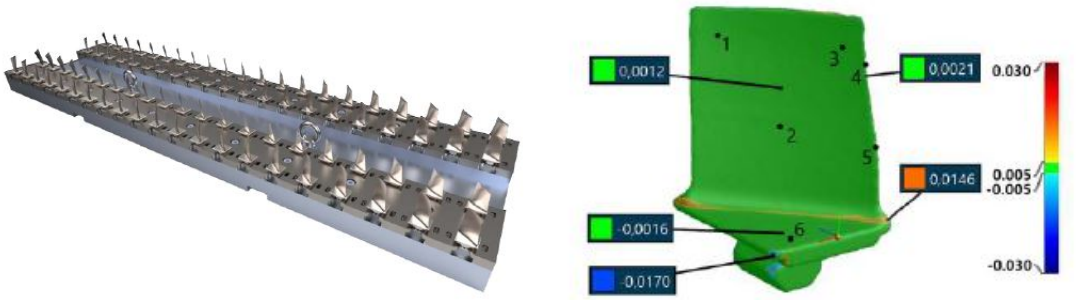

(a) Fixture model. (b) HPC blades point selection for measurement.

Figure 4.8: Developed work on HPC rotor blades [16].

This thesis has the same objective of creating a measuring process of engine components. However, this study is focused on LPT nozzles that, like HPC rotor blades, influence aerodynamically the engine performance.

4.3 LPT Nozzle Dimensional Inspection

Currently, the engine maintenance shop in TAP M&E does not have a process to measure the discharge area of LPT nozzles. The manufacturer does not provide geometric parameters to compare with the measured parameters. With this in mind, it is relevant to design a method to measure LPT nozzle's exit flow area and relate it to the engine performance tested in the test bench. Thus, it is possible to predict engine behavior and improve engine maintenance in more effective progress.

Keeping this in mind is important to determine a process to inspect NGV's in terms of geometric parameters. There is a study by Rolls-Royce members that analyze geometric variations in NGV [9]. In this article, the design process of measurement goes through the steps represented in Figure 4.9.

Creating a CMM program to measure the exit flow area is a reverse engineering process. It is a complex and time-consuming process based solely on the workpiece in its physical state. In the various steps that make up this process, several areas of engineering

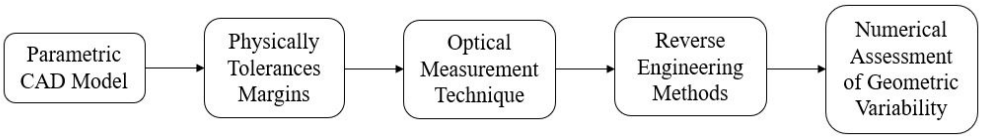

Figure 4.9: Design Process of Meyer M. [9].

will be addressed, and various pieces of equipment that are indispensable for obtaining a credible final result to be in production will be used.

Given the complex geometry of the part under study and since it is a non-prismatic part, it is impossible to create a CAD model using basic measuring instruments. A high-precision laser scanner - HandyScan Laser Scanner - is required to generate the first digital model as a mesh. This mesh will then be used in SolidWorks as a reference for developing the CAD model of the nozzle.

The model generated through the scanner presents a refined mesh that SolidWorks cannot process. Therefore, using MeshLab to rework the mesh, can reduce the number of mesh nodes without compromising the accuracy of the area under study (exit flow area). With the optimized mesh model, building the parametric model in SolidWorks that coincides as much as possible with the mesh is possible. Once the parametric model is developed, a body comparison between the developed model and the refined mesh is performed to verify its accuracy since this operation is performed by VXelements, with a high mesh processing capacity. It is possible to proceed to the next steps by verifying the high approximation between the parametric and the physical model.

The clamping tool is developed in order to guarantee the static condition of the nozzle concerning the CMM. In this design, it is essential to consider the calculation of the external forces applied, as well as the tolerancing of the contact surfaces.

The fact that there are no references about the exit flow area from the manufacturer makes it necessary a reverse engineer process to obtain the sections that define these areas. In order to have reference values, two nozzles were sent to the manufacturer to be measured in CMM.

5

Scan and Modelling

As seen before, in order to create a 3D CAD model of the nozzle is necessary to generate a reference mesh model using a 3D scanner like the Creaform HandySCAN 3D.

5.1 Scan and Reference Model

To scan this nozzle is necessary to digitize different viewpoints to acquire the minimum set of points that define the shape. The first step of the process is to attach positioning targets to the rotating plate to provide more accurate results and to permit that during the scan, the part can rotate and align instantly. This rotation permits digitizing multiple viewpoints and obtaining a set of points that define the shape. The positioning targets work as reference points and permits the software *VXelements* to locate those points and align the part with more accuracy. The scanning workspace is represented in Figure 5.1.

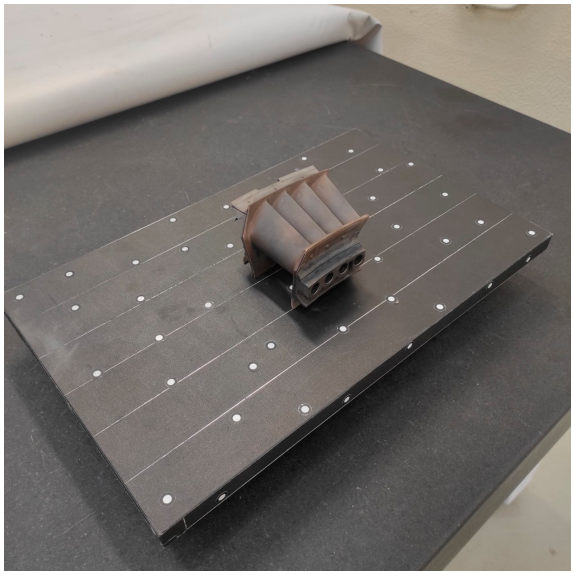

Figure 5.1: Scanning workspace.

Making sure that the scan is aligned in all instances is mandatory to guarantee that there are at least three targets within the projection of the light stripe pattern. It is

recommended by *VXelements* manual that the positioning targets must be applied with a distance between 100 mm and 200 mm from each other.[11]

Some factors as pressure or temperature variations, can change the mechanical configuration of the scanner. To maximize the quality of the results and according to the manual specifications, it is advised to calibrate the scanner using the calibration plate each time it is used. Within this scope, a calibration was made, and proceeded to the first scan. During the scan is essential to maintain an optimal distance between the scanner and the part around 40cm.

In this case, to obtain a complete set of points that define the shape is necessary to make four distinct scans with the part laid in four different positions. Between each scan is mandatory to merge the scans to obtain a mesh surface with coincident zones with points common to both scans and zones that were not detected in the previous scans.

The alignment method used was the best fit. This method permits merging different scans into a single mesh. Best fit alignment uses an iterative closest point algorithm called the least-squared method, where the sums of squares of points distances between the surfaces are minimized. [18]

There are difficult zones to scan, as in the three surfaces between the vanes. This adversity is related to the lack of light in these zones. Even though it is possible to operate the scanner in any position, no angle captures points in these surfaces. This impossibility leads to the formation of holes.

In *VXmodel* there are mesh processing tools that correct possible mesh defects such as irregularities, spikes, and holes. After merging all the scans into a single mesh, a command was used to clean and delete any captured points that did not belong to the part, such as points captured on the rotating plate.

To generate a surface that fills a hole, the 'fill holes' command of *VXmodel* was used. This fulfillment presents deviations concerning the physical model. It will be seen in the next section that those deviations do not influence the CAD model accuracy. The location of one hole is represented in Figure 5.2. The other two holes were located in the same zone and were fulfilled using the 'fill holes' command.

5.2 CAD Model

The CAD Model was developed using the *SolidWorks* software which is compatible with the scan software. The STL file generated in *VXelements* is opened by *SolidWorks* imported as a surface body. (This surface body (instead using solid body) permits the reduction of the file size resulting in the shortage of processing time.)

The nozzle can be divided in three distinct bodies taking into account the construction of the CAD model: outer platform, vanes, inner platform.

The design of this model is always based on the primary purpose of measuring the discharge area with a CMM. Taking this into account, there are functional surfaces that are relevant to developing the program for the CMM, and there are non-functional

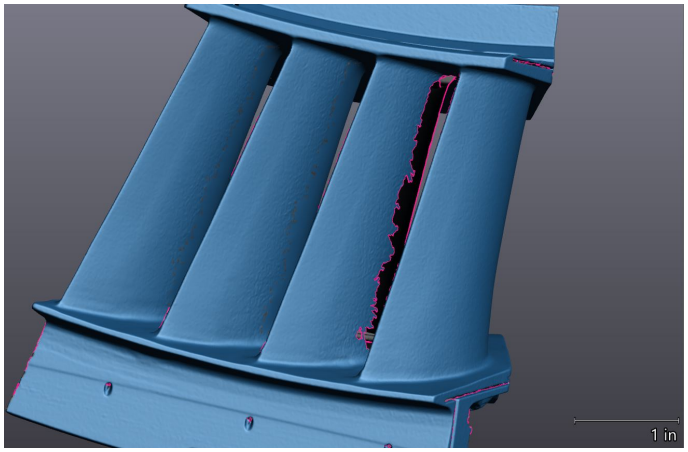

Figure 5.2: Location of holes.

surfaces which is the case of cooling slots in the outer platform. Non-functional surfaces will not interfere with the measurement process and can be ignored when developing the CAD model.

Some dimensions defined in the Engine Shop Manual from CFM are helpful in the construction of the CAD model since some dimensions are related to functional surfaces. Specifically, the dimensions D, E, and G from Figure 5.3 will be taken as a reference in this model.

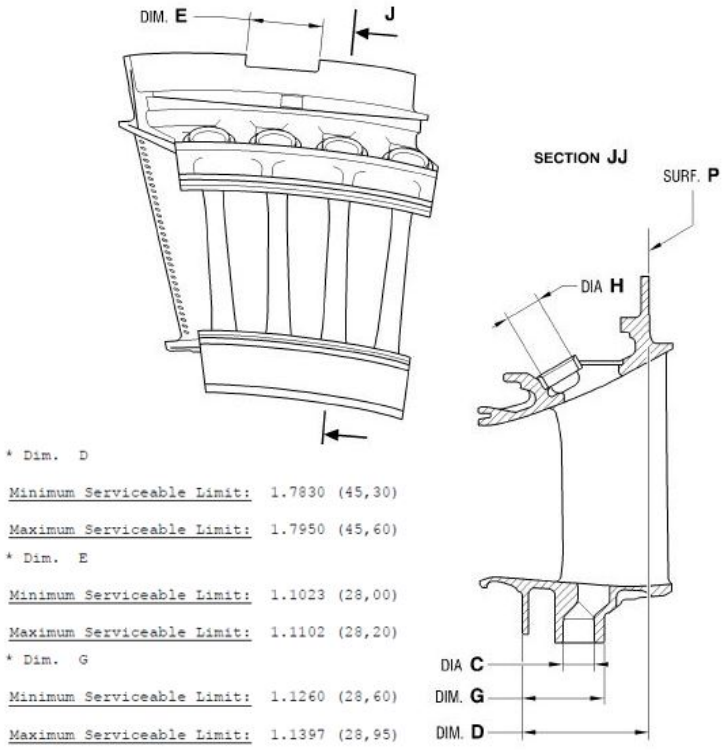

Figure 5.3: Dimensions from CFM's Engine Shop Manual, [19].

Functional surfaces can come from three different natures:

- Surfaces that will directly be measured by the CMM, such as the vanes surfaces;
- Seating surfaces for the fixture tool;
- Alignment surfaces for the CMM program.

Considering that is going to be used a scrap nozzle for the reference model, this CAD model will have deviations relative to the original dimensions. However, in a maintenance environment, all the nozzles that will be measured will have deformations associated with operation times. So this model turns out to be closer to those measured later in the CMM.

During the construction, the CAD model should overlap the reference model considering some mesh irregularities. This will be done by creating sketches with points coincident with vertices from the mesh.

The first step of this process is to create planes that permit the generation of the three bodies (outer platform, vanes, inner platform). Since this nozzle is a revolved part is necessary to find the revolution axis and create the plane that will permit drawing of the sketches to generate the outer and inner platforms. The revolution axis was found with three point arc sketches overlapping edges that are in contact with the HPT shroud. The axis localization was confirmed using a diameter tape, measuring the diameter of the LPT nozzles set and comparing with the CAD model. In Figure 5.4 is possible to see the value of 33,3 inch that corresponds to 845,28 mm, i.e., a radius of 422,6 mm. The same measured surface in CAD model has a distance of 413,8mm to the revolution axis, which confirms crudely the axis localization. This disparity in values is acceptable as long as the parametric CAD model is sufficiently coincident with the reference mesh model. The model accuracy will be analyzed in the next section.

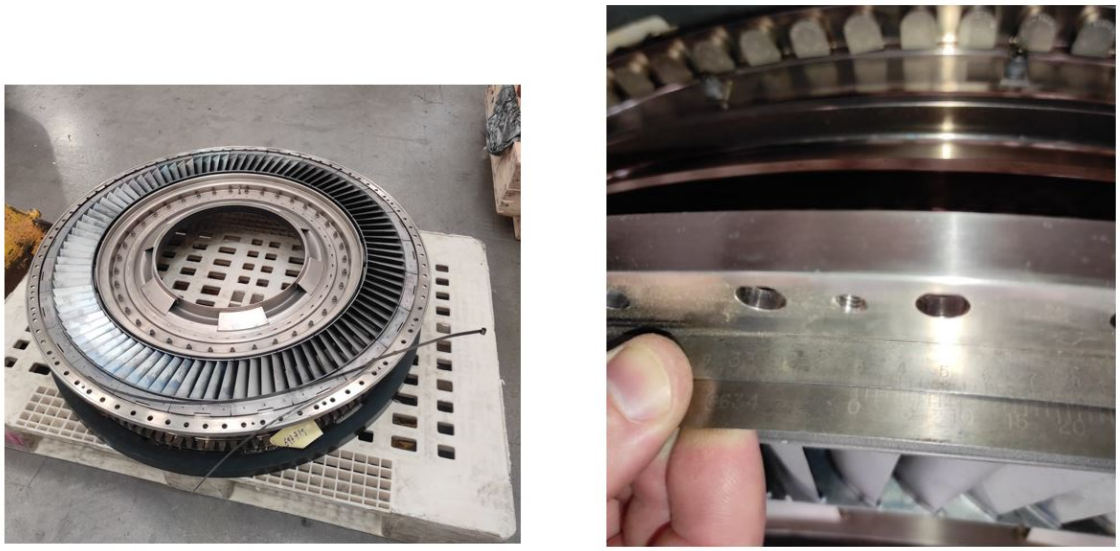

(a) Measured diameter.

(b) Value of the diameter in *inch*.

Figure 5.4: LPT nozzle set diameter measure to locate the revolution axis.

So the outer and inner platform are created from the revolution of the sketches, represented in Figure 5.5, around revolution axis.

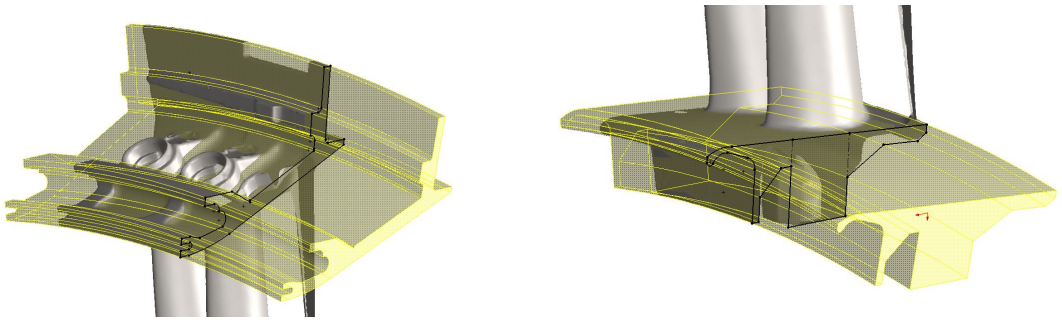

(a) Outer revolve platform sketch. (b) Inner revolve platform sketch

Figure 5.5: Construction of outer and inner platforms.

In order to cut the excess of the platform body, that is notable in Figure 5.5(a) on the left side, it was created planes perpendicular to the radial direction. With these planes generated is possible to create sketches that will cut the platform with the right direction.

As was said before, in the reference model, some vane shapes present deviations concerning the physical model due to the fulfillment of holes generated by the software *VXmodel*. Since all vanes have the same geometry, it is possible to design them just with two surfaces from the tip vanes. Regarding the scan, one tip vane has complete visibility of the suction surface, and the other has complete visibility of the pressure surface. This means that the reference model presents high accuracy in these zones and is possible to construct the vanes with these two surfaces.

With this being said and being aware of the exit flow area location that has been seen in Figure 3.5, vanes modeling was made based on the tip vane that has the suction surface full visible.

The vanes modeling proceeding starts with creating planes with the intention to generate a loft. It was decided to create ten planes to obtain an accurate loft that define the vane shape. The ten sketches that define the loft are represented in yellow in 5.6(a). For each plane it was created a section view and was drawn a sketch that overlapped the reference model. In Figure 5.6(b) is possible to observe one example of a sketch.

The sketches are made through several arcs that will define a closed contour corresponding to the section of the vane in that plane. At first, these sketches were made using splines defining several points along the contour of the section, which on the one hand, results in a highly accurate overlap of the sketch with the reference model, but on the other hand, makes the construction of the loft and some adjustments that have to be made after the construction more complicated. With arcs defined through radii of curvature, it is possible to change only the dimensions associated with the radii to correct some deviations that may occur later. To generate the loft is essential to define all sketches with

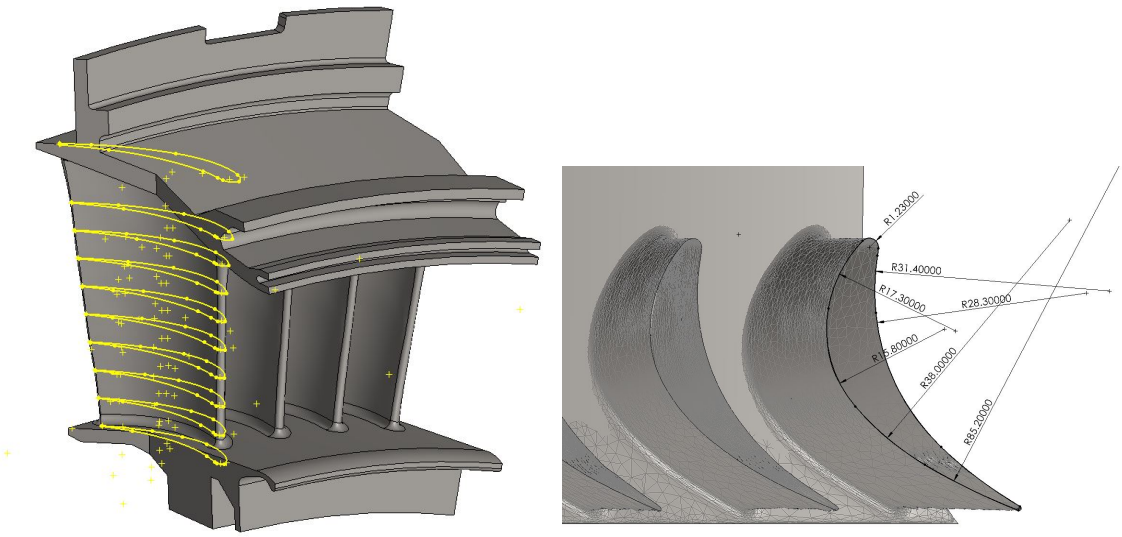

(a) Sketches that define the vane loft

(b) One sketch that define the loft.

Figure 5.6: Vane loft construction.

the same amount of arcs (10 arcs for this case) and ensure that the extremities are located in the same zone in all sketches.

A circular pattern was made concerning the axis of revolution to create the four vanes equally spaced. The angle between the vanes was determined by trial and error with the aim of overlapping the vanes of the CAD model with the reference model. The last step was to create the fillets between the vanes and the platforms.

It is essential to consider a factor that the machine operators recommended about the CAD model regarding the presence of edges in the airfoil. The format of the CAD file that *MCOSMOS* can read is STEP, when converting a SolidWorks file to STEP, when there are edges on the airfoil, *MCOSMOS* interprets the airfoil as two distinct surfaces which will make it challenging to perform the measurement program on the CMM. Therefore, it is necessary to ensure that in all sketches that define the loft, all the radii of curvature are tangent to each other to generate only one surface that constitutes a vane.

5.2.1 CAD Model Accuracy

As was said before, functional surfaces are crucial to the further steps of the measurement process. These functional surfaces should match the reference model and the CAD model with deviations below 0,02 inch. This value is an empirical value that was advised by *Técnico de Manutenção Aeronáutica* (TMA)'s so that there would be no problems later on with the CMM program.

In the interest of comparing the CAD model and the reference model, the command "Body Compare" from *VXmodel* was used. This command permits merging two bodies, in this case, a CAD model and a mesh surface, and analyzing the deviations between

these two bodies. This command permits an accessible reading of the deviations since it is represented with a color map. The color scale goes from 0,394 inch to -0,394 inch. In Figure A.1 and A.2 are represented some deviations from the body compare and the color scale.

The first thing to notice is the cooling slot zone, where the deviations are massive. This zone is represented in pink in A.1. As was said before, the cooling slots are non-functional surfaces, so the deviations in these zones can be ignored. Another critical point is the propagation of the deviation along all vanes. It is possible to notice a deviation pattern in each vane. This phenomenon happens due to how the CAD model was built, notably the vanes modeling, where a circular pattern was used based on only one vane.

In general, is possible to notice the presence of a lot of green surfaces, which represent residual deviations, and some yellow and blue zones that represent deviations within the allowable values of 0,02 inch.

6

Fixture Design for Dimensional Inspection in CMM

Continuing the work developed by Farinha E. [16] and Rendas P. [13], it is of great interest for TAP M&E to possess a fixture tool for the CMM's measurement process of the nozzles exit flow areas.

The development of this tool allows the creation of a CMM program and establishes an effective measurement process with minimal labor requirements by the operator. This efficiency is guaranteed through the most autonomous measuring process possible using the equipment available in the engine shop. The main objective is to ensure the tightness of the nozzle in the same position for every measurement with the target of minimizing the processing time.

The design method used is based on Axiomatic Design Theory. Based on the customer needs, TAP M&E, the functional domain has the Functional Requirements (FR), which are the minimum set of requirements a system must satisfy, and the physical domain with the Design Parameters (DP), which are the vital physical variables that characterize design solution. The DP are the response for the FR to integrate physical entities and develop an intricate system - the fixture tool. However, first is critical to keep in mind the principles of fixture systems.

6.1 Principles of fixture systems

During an inspection operation, fixtures are commonly used to ensure repeatable positioning and orientation of the workpiece concerning the instrument or tool being used, which in this case is the CMM. A well-constructed and planned fixture ensures the predictable location of a workpiece, which benefits the production environment by increasing part repeatability, lowering cost per unit, and improving overall end product quality. [20]

Every item is assembled using a system that creates and maintains an interface between a workpiece and an end effector, in this case, is the contact between the nozzle and fixture tool. Depending on the component or system used, the interfaces perform two essential and two optional functions. In table 6.1 are represented the four functions of

interfaces in a fixture system. [20]

Table 6.1: Functions of interfaces in fixture design.

Essential Functions	**Description**
Location strategy	To position and orient the component in space strategically.
Clamping strategy	To keep the component in place against any external forces by removing the appropriate degrees of freedom.
Optional Functions	**Description**
Support strategy	To reduce the part's deformation throughout the inspection process.
Tool interaction	To guide or interact with the process end effector.

Additive Manufacturing (AM) can be used to construct prototypes for design evaluation since is a technology capable of producing parts with complex shapes rapidly with reduced costs. In this thesis is going to be used AM technology to verify dimensions and check geometric tolerances.

There are mainly two types of fixtures: modular fixtures and dedicated fixtures. A modular fixture is proper to accommodate different geometric types of components. For complex geometric components is needed a combination of various elements to compose a fixture. The dedicated fixture is designed for a single component with an extensive product volume. Since this thesis is dedicated to measuring exit flow areas of a LPT nozzle from one specific engine (CFM56-5B), the dedicated fixture is the most viable option.

6.2 Functional Requirements

Tool fixtures are used to ensure the repeatable position and orientation of the workpiece in a mass inspection. In this case will guarantee the improvement of dimensional inspection capability. To develop the fixture it must be settled well-defined FR in order to meet all the measure process specifications. There are three main FR for this design:

- Immobilizing the nozzle in a kinematic analysis;
- Reducing operation time;
- Guaranteeing the repeatability and locating accuracy.

Guarantee immobility in terms of kinematic analysis translates in constraint all DoF. This constraint is assured by the fixture tool, where snapping the nozzle in the tool should be fast and easy from the operator's point of view. A reduced operation time translates into a high inspection rate which is a customer need. The accuracy related to repeatability

is related to how the nozzles are mounted on the engine. In Figure 6.1 is illustrated one set of LPT nozzles mounted. To measure the exit flow areas of the tips is necessary to have two reference nozzles, one on each side, to lean against the nozzle to be measured. It is important to notice that there is a gap between nozzles that must be considered when developing the fixture.

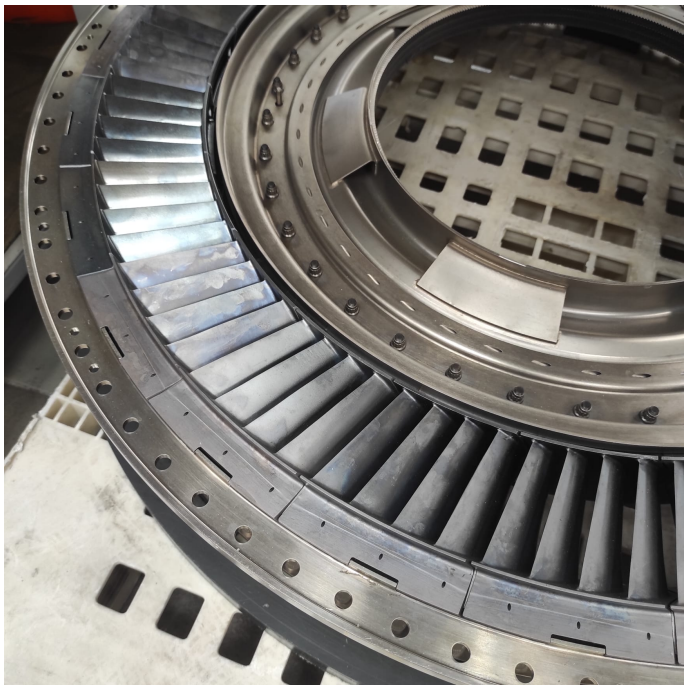

Figure 6.1: Set of nozzles mounted.

6.3 Design Constraints

Design constraints are an obstacle between the functional requirements and the design parameters. These constraints are mostly related to budgets and equipment limitations.

The fixture was developed without considering the expense. Nevertheless, in accordance with proper design procedure, cost reduction will be taken into account while developing the tool without sacrificing the quality. It is essential to consider manufacturing difficulties during the design, which can turn the manufacture of this tool too expensive. This design considers that the tool will be manufactured using a Computer Numerical Control (CNC) machine.

When it comes to equipment limitations, it is critical to consider some equipment characteristics. The fixture tool function is to fix the nozzle properly to be measured in the CMM, where the tool stands in the granite bed.

The fixture must fit in the CMM work volume, but this is not considering the probes movement and access to the probe's tree. These considerations were made in Rendas P. [13] whose the fixture developed is being used in engine shop. To the previous considerations adding the CMM's arm and the probes stylus dimensions, Rendas P. contemplated

on his study a conditioned available volume to develop the fixture of 700x900x1000mm, represented in Figure 6.2. Since the tool developed by Rendas P. is currently used at TAP and performs well, it is going to take to account this volume to develop the fixture.

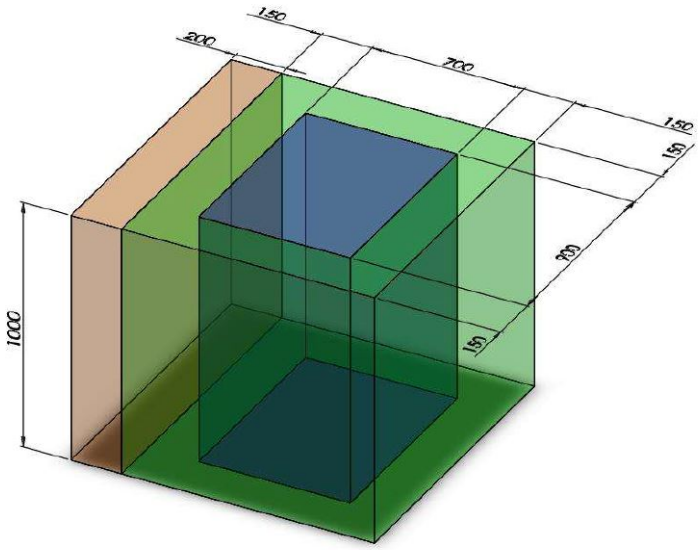

Figure 6.2: CMM available volume to fixture design.

When assembled, the fixture tool must not damage the nozzle's serviceability or leave any marks. That being said it is going to be used the minimal forces possible to fix the nozzle to prevent material deterioration.

Before doing any tool design, it was insisted a meeting with the TMA's in order to design a solution that would be reliable in terms of manufacturing. Crucial aspects were discussed, such as: using as few parts as possible, trying to decrease the use of manufacturing tolerances, and, with CNC manufacturing in mind, using aluminum as the base material for the tool. Several types of aluminum were discussed, and the conclusion was reached that the 7075 aluminum was the one to be used. Comparing this aluminum with other types, this one was chosen because of its high ultimate tensile strength (recommended for structural parts), improved stress-corrosion cracking resistance, and the fact that it is often used in aircraft fittings. Another advantage is that TMA's are used to work with this type of material.

6.4 Design Parameters

Now that the fixture tool design has been appropriately introduced, the next stage consists of the construction of the various tool features that fulfill all the FR while respecting the design constraints mentioned in the previous section.

In this section it is going to be discussed the physical features that gives the answer to the FR which includes the nozzle set configuration, the fastening system and the easy-to-fit method.

6.4.1 Nozzle Set Configuration

The position in which the nozzle is fixed on the tool has a significant influence on the efficiency of the measurement process. It is crucial to establish a single position that allows all five areas to be measured at once and guarantee a set where planar surfaces are parallel to the granite bed. The exit flow areas to be measured are located close to the trailing edge (the exact position of each will be seen in the following chapter).

With that said, the nozzle orientation is arranged with the leading edge facing the granite bed and the trailing edge facing upwards to allow the probe full access to the exit flow areas. It is crucial to guarantee that in this disposition, the surfaces that are in contact with the HPT shroud when the nozzle is mounted are parallel to the granite bed to simulate the nozzle set mount configuration. These surfaces are represented in Figure 6.3.

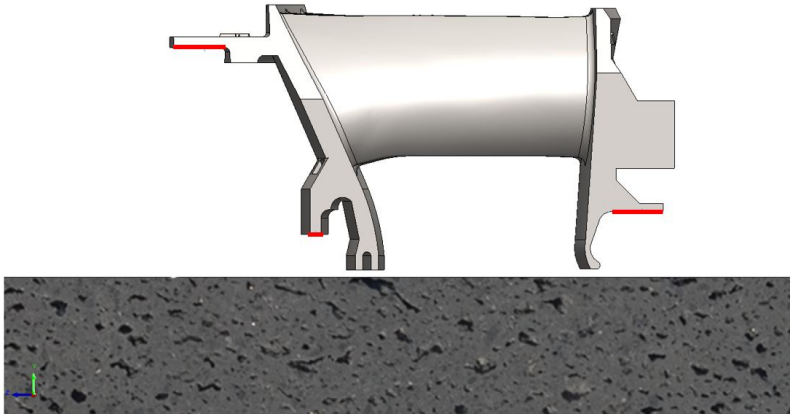

Figure 6.3: Parallel surfaces with the granite bed that contact HPT shroud.

The orientation of the nozzle in the CMM referential is represented in Figure 6.4, with the simulated approach of the probe.

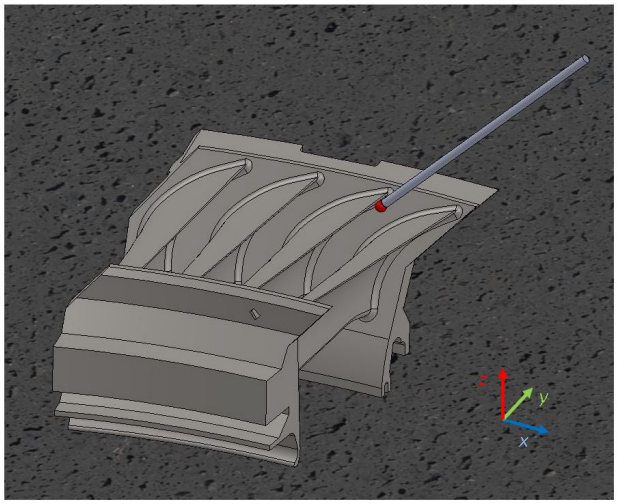

Figure 6.4: Nozzle orientation in the CMM referential.

By simulating the probe's approach to the exit flow area, it is possible to verify the presence of difficulties that may occur during the measurement. The measurement occurs with the probe traveling along the perimeter that defines the exit flow area, thus generating a closed contour of that area. Is important to note that the probe must also go through the fillet zone to generate points referring to this radius of curvature. This leads to a limiting factor regarding the choice of the probe to be used. As seen in Table 4.1, the RSP2-3 has a 3 mm radius sphere and the RSP-3 has a 2 mm radius. Having measured and defined a radius of curvature of 2,2 mm for the concordance between the airfoil and the platforms, and after analyzing the CAD model through the body comparison present in the Appendix, is possible to verify that this zone is green i.e. the nozzle presents a fillet of approximately 2,2 mm. This rules out the possibility of using the RSP2 probe for this study since the tip presents a radius of curvature of 3 mm, which would be impossible to obtain points in this zone, as can be seen in Figure 6.5.

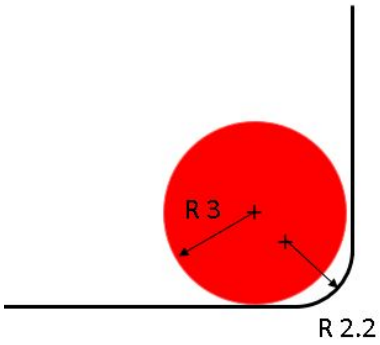

Figure 6.5: RSP2-3 probe radius impossibility.

Although the exact position of the exit flow area is not known, we know from chapter 3 that it is located near the trailing edge in a plane more or less perpendicular to the inner surface of the airfoil. From Figure 6.4 and after having a notion of the geometry of the nozzle is possible to verify that the deeper the probe is, in relation to the trailing edge, the more difficult is to obtain a fixed angle θ that allows the probe to travel through the patch defining the exit flow area.

Is it possible to define a maximum angle θ and a minimum angle θ that delimit the possible angle to execute the measurement, fixing the β angle. These θ angles are obtained using *Solidworks*, by making an assembly simulation with the nozzle model and a probe model. In this assembly are defined mates that allow simulating of the probe scanning along the contour, i.e., ensure contact between the sphere of the probe and the airfoil surface and also define an angle θ and check if there are interferences (using the command "Interference Detection") between the probe stem and the part. Due to the geometry of the nozzle, the critical position to define a minimum angle β is when the probe is located in the corner, as seen in Figure 6.4. With a fixed angle, β of 180 degrees, the minimum θ angle possible is represented in Figure 6.6.

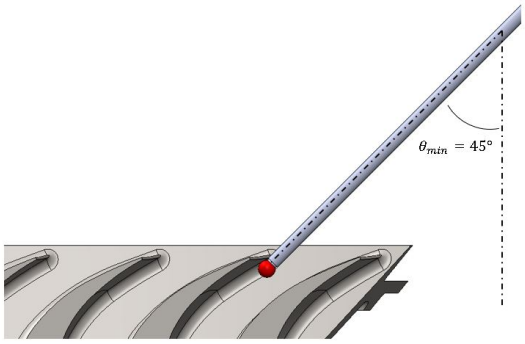

Figure 6.6: Minimum θ angle.

With the same fixed angle β of 180 degrees, the maximum θ angle possible is represented in Figure 6.7.

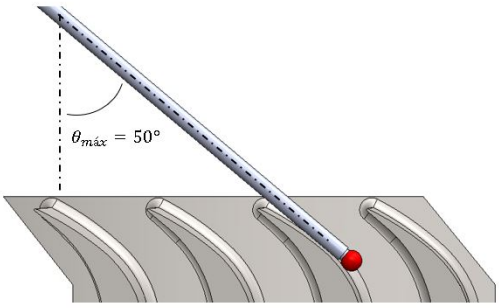

Figure 6.7: Maximum θ angle.

Notice that those Figures above are images of the section view parallel to the yz plane. With this, it can be concluded that for this arrangement of the nozzle in the CMM, there is a range of possible angles, with $45° < \theta < 50°$, where only the sphere can be in contact with the surface during the measurement.

The main goal of this study is to measure the exit flow areas of a nozzle, with a view to making this measurement for the entire set of 24 nozzles. With this in mind, it is crucial to decide which areas will be measured in a nozzle.

There are two approaches to this decision: measuring the three exit flow areas that can be measured directly between two vanes of the nozzle or somehow including these three areas, the associated tip areas between the tip vanes of that nozzle and the previous and subsequent nozzle tip vanes. If the first approach of measuring only the three areas of each nozzle were used, it would not be possible to obtain the value of all the areas of a set of nozzles. Since the set consists of 24 nozzles, all areas between nozzles would remain to be measured, i.e., 24 output areas would remain to be analyzed, which can significantly influence the engine's efficiency. Therefore, it is necessary to include the five exit flow areas in the measurement process. In order to be able to measure the tip exit flow areas, it is necessary to simulate the nozzle set mount configuration in the engine

and add two nozzles, one on each side of the nozzle, in the study.

The nozzles that will serve as an aid for measuring the tip areas will always be the same for all measurements. They will be nozzles that do not belong to the set, and as they are always the same, they become the master nozzles and coherent with the process of obtaining the tip areas. So the final nozzle set configuration will look like the Figure 6.8.

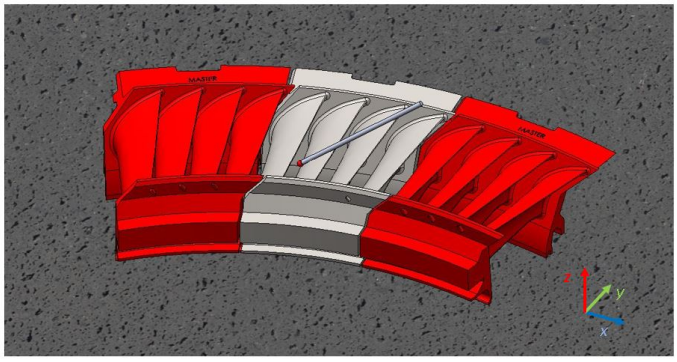

Figure 6.8: Final set configuration.

Notice that there is a clearance between each nozzle that in Figure 6.8 is exaggerated but can be seen in real terms in Figure 6.1. The master nozzles are represented in red.

In order to determine the clearance between the workpiece and the master nozzles, to be assigned in the operating condition, a manual test was performed using a feeler gauge in which all the 24 gaps of an available set were measured. The determination of the gaps is done by trial and error, and the clearance values for the 24 gaps are represented in Table 6.2.

Table 6.2: Sample values of the clearances.

Number of Gaps	Clearance [inch]
4	0,04
18	0,05
3	0,06
Average	0,0496

It was determined that the average clearance in a set of nozzles is approximately $0,05 inch$. For each operation this clearance is ensured by positioning a feeler of $0,05 inch$ between the nozzles at the time the set-up is mounted, like is demonstrated in Figure 6.9. The operator slides the nozzle until touch the filler plate and then the ball plungers "hold"the nozzle in place.

In terms of functions of interfaces in fixture design described in Table 6.1, the location strategy is defined.

Figure 6.9: Method to measure clearance between nozzles segments.

6.4.2 Fastening System

In space, a body has six DoF. Every motion is entirely determined by its three-dimensional directions and three axes of rotation. If these six motion components are halted, the body cannot move and all degrees of freedom are eliminated. The elimination of the six DoF is done by the 3-2-1 principle. This principle is represented in Figure 6.10.

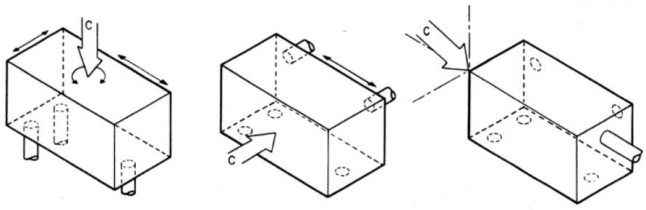

Figure 6.10: 3-2-1 principle, [21].

Three non-straight-line points are assumed to operate with a hold-down pressure on the block, preventing it from being lifted off in the vertical direction. These three points restrict vertical motion and rotation across a longitudinal and transverse axis. The block may still move in two directions and rotate along a vertical axis in the plane defined by the three points. With two points on the side surface, not in the same vertical line, and again with associated hold-down pressure, the block is prevented from moving in the crosswise direction and rotating around the vertical axis, depriving it of two degrees of freedom. It has one degree of freedom remaining, and one locating point against the end eliminates the sixth. [21]

In order to define the fastening system, it is necessary to define the seating surfaces that will represent the first three points that define a plane, and the surfaces that will serve as a guide to install the nozzle in the tool will define the following two points. A

stopper achieves the last point that eliminates the sixth degree of freedom. The hold-down forces, represented with C in Figure 6.10, are achieved by a clamping mechanism that will be seen in more detail later.

The necessity to set the nozzle with planar surfaces parallel to the granite facilitates the allocation of the seating surfaces in the fixture. In Figure 6.11 is possible to see the seating surfaces (represented in blue) that, in conjunction with the C force, will eliminate three DoF, associated with Z direction movement and the rotational motions about the Y and X axes (CMM referential). In Figure 6.1 it is possible to have the notion that these surfaces are in contact with the HPT shroud when the nozzle is mounted.

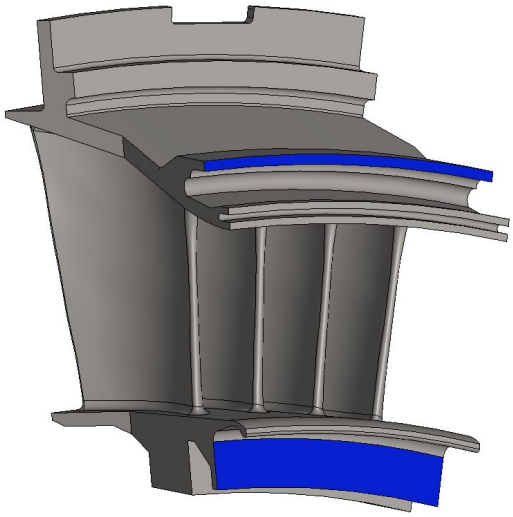

Figure 6.11: Seating surfaces.

The need for a guiding mechanism depends on each operation's precision. The fact that the assembly is guided decreases operation time and increases accuracy concerning the position. Since the nozzle will slide between two guide surfaces, this contact will eliminate two DoF associated with the rotation of the part to the Z axis and the motion in the Y direction. The guided surfaces of the nozzle are represented in green in Figure 6.12.

The last DoF associated to the motion in the X direction, is eliminated with a stopper that must be included at the end of the guide surface.

With the guide surfaces and the seating surfaces well-defined, it is possible to get an idea of the geometry of the base of the fixture. In order to simulate the set mount condition of the nozzles, the tool is developed against the background of the HPT shroud where the nozzles are mounted. The first design condition is the distance between the seating surfaces, represented in Figure A.4.

The other crucial geometric parameter is the distance between guided surfaces. The curvature radius of these surfaces as a first approach will not be considered dimensional tolerances because it will be considered later in this chapter. The curvature radius of the guided surfaces is represented in Figure A.3.

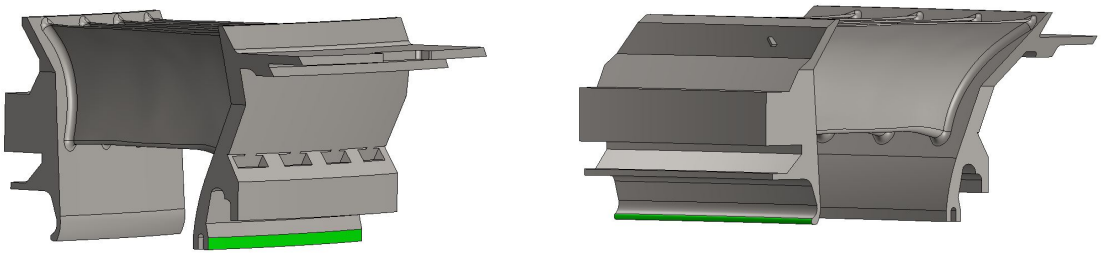

(a) One guided surface.

(b) Another guided surface.

Figure 6.12: Guided surfaces.

With this in mind, the first stage of the base fixture looks as shown in Figure 6.13. In this first approach, the guide surfaces present the same curvatures as the guided surfaces and the same center as seen in Figure A.3. The guide surfaces are represented in green, and the seating surfaces in blue. The seating surface's height is shown in Figure 6.13. Those height dimensions were determined by ensuring that only the seating surfaces touched the fixture tool. The length of the curvature is determined by ensuring that three nozzles, next to each other, fit in the tool.

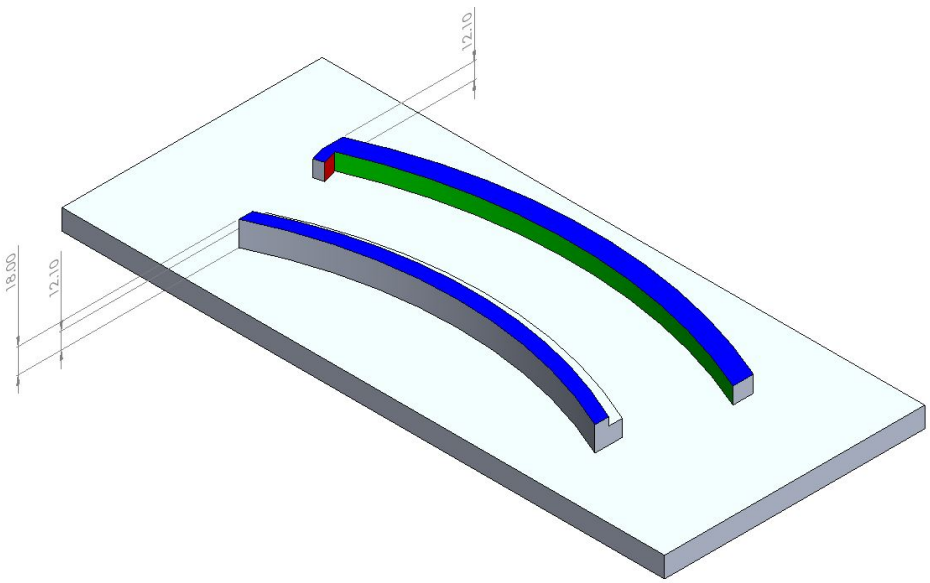

Figure 6.13: First stage of the base fixture.

The radius of $2mm$ is a facility in terms of manufacturing and can be changed according to the milling cutter available in the CNC machine. The stopper is added to the outer guide surface to stop the nozzle when the operator is sliding the nozzles to fix them, eliminating the last DoF. The stopper is represented in red in Figure 6.13 and can be seen in more detail in Figure 6.14. This stopper was designed to guarantee the coincidence

between the stop surface and the nozzle surface under the condition that the green surfaces are in contact. In order to facilitate contact between surfaces and manufacturing difficulties, it is necessary to avoid sharp corners. With this in mind, the presence of an indentation will resolve both adversities.

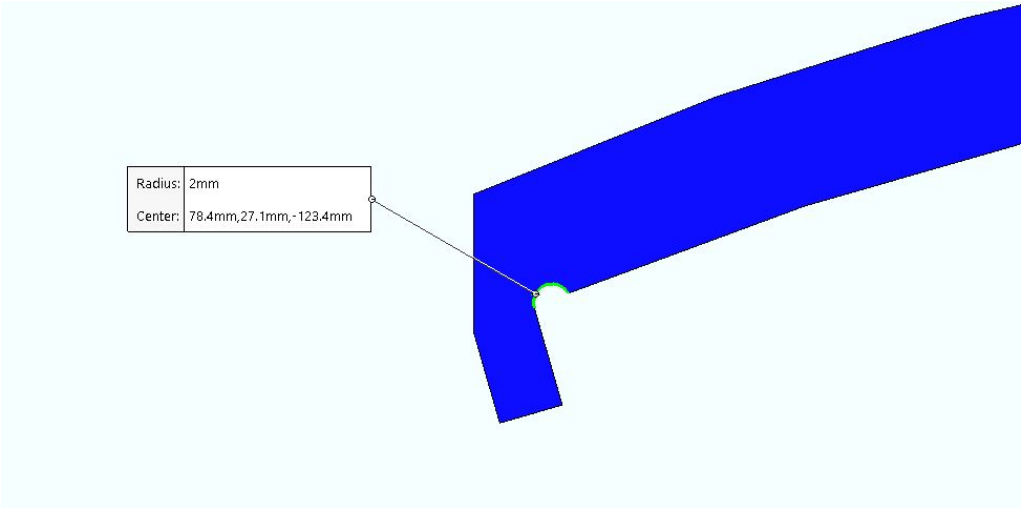

Figure 6.14: Stopper radius detail.

The 3-2-1 principle always assume hold-down pressures against the surfaces where the points are defined. The forces that provide this pressure will be insured by ball plungers [22] represented in Figure 6.15 and the frictional force generated by the weight of the nozzle. These plungers are to be inserted along the guide surfaces in order to create the necessary pressure to block all DoF.

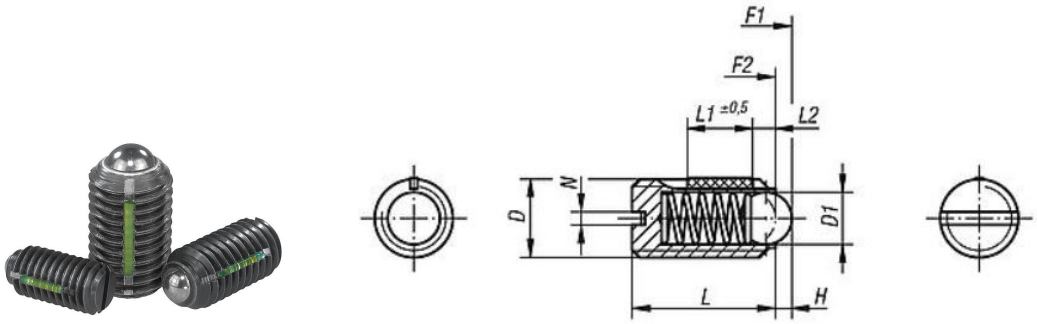

(a) Ball plunger aspect.

(b) Ball plunger section view.

Figure 6.15: Ball plunger.

Apart from generating a hold-down pressure, ball plungers provide a mounting facility. When sliding the nozzle into the tool, the ball plungers will compress and ensure that the workpiece touches the surface opposite to where the balls are located, i.e., the balls will push the nozzle against the other guide surface and ensure the position without the use of a screw clamping mechanism. The mechanism with the spring excludes the need for tight tolerances since the deformation of the spring itself will take into account any

gap between surfaces (that will facilitate the manufacturing process).

These plungers are available in different sizes where all the parameters represented in 6.15(b) change. These specifications are represented in Table 6.3.

Table 6.3: [22]

D	L [mm]	H [mm]	F1 [N]	F2 [N]
M3	7	0,4	1,5	3
M4	9	0,8	4	10
M5	12	0,9	6	11
M6	14	1	9	13

When the operator inserts the nozzles into the guides, the force exerted on the part to slide will be transferred to a force associated with the deformation of the spring inside the plunger. This deformation is associated with a compression force of the spring against the nozzle surface, which will generate friction between surfaces. The frictional force generated will guarantee no movement of the part in question during the measuring operation. That is, all DoF are eliminated.

6.4.2.1 External Forces

In order to determine the hold-down pressures required to immobilize the nozzles, it is necessary to take into account what external forces are possible to occur during the measurement process. The forces that occur during the process are the force exerted by the probe and the gravitational force. Forces caused by accidents of the operator will not be considered because if during the measurement any contact occurs between the operator and the workpiece, this operation is invalid.

It is necessary to determine the force exerted by the probe to evaluate what forces are required to ensure the static condition of the nozzle. As seen before, the probe that will use is the RSP3-2 from *Renishaw*. This probe works with a touch trigger mechanism associated to a spring. After consulting the specifications from the manufacturer manual, it becomes possible to calculate the force exerted by the probe. These specifications are represented in Figure 6.16.

Probe attributes	Scanning with 3-axis measurement (X, Y, Z) and 3-axis touch-trigger	
Measurement range	±0.5 mm deflection in all directions in all orientations	
Overtravel range	X, Y	2 mm
	+Z	1.7 mm
	-Z	1.2 mm
Resolution	Capable of <0.1 µm	
Spring rate	Nominally 0.6 N/mm - when using shortest specified stylus Nominally 0.2 N/mm - when using longest specified stylus	

Figure 6.16: RSP3 specifications, [23].

To calculate the force exerted by the probe, it is necessary to consider two parameters: spring rate and overtravel range. Note that the overtravel range in Z differs depending on the direction of movement in that axis. In Figure 6.17 is possible to have a notion of the touch trigger mechanism. On the right side is represented the force balance when the overtravel occurs in X or Y direction, and on left, the overtravel occurs in Z direction.

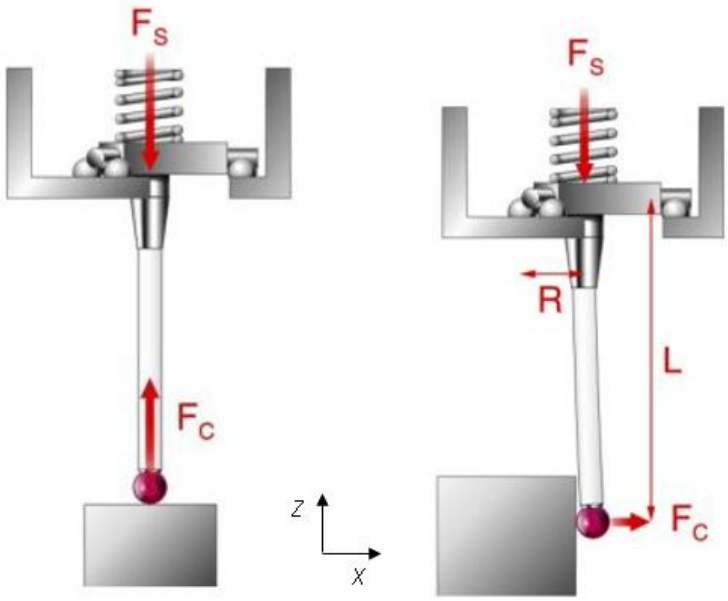

Figure 6.17: Force diagram, [23].

In Figures 6.7 and 6.8 it is possible to see that the probe will move with its axis perpendicular to the surface where the sphere is in contact. This way it is verified that the force that the probe will apply will be in the X or Y direction. Proceeding then to calculate the external force applied by the probe in relation to the X direction, the following equilibrium equation (established by the manufacturer) is [23]:

$$F_C \cdot L = F_S \cdot R \tag{6.1}$$

For a displacement in the X or Y direction, $\delta_{X,Y}$ there is a deformation in the spring associated to a displacement $\delta_S^{X,Y}$. Similar to the force balance, $\delta_S^{X,Y}$ is given by:

$$\frac{\delta_{X,Y}}{L} = \frac{\delta_S^{X,Y}}{R} \tag{6.2}$$

The values of L and R are depicted in Figure 6.18.

For a maximum displacement of $2mm$ and $L = 130mm$ and $R = \frac{25}{2} = 12,5mm$, it comes:

$$\delta_S^{X,Y} = \frac{2 \times 12,5}{130} \simeq 0,2mm \tag{6.3}$$

This displacement does not cause a linear spring deformation, i.e., where the displacement is calculated at the end of the base where the spring is seated. This displacement

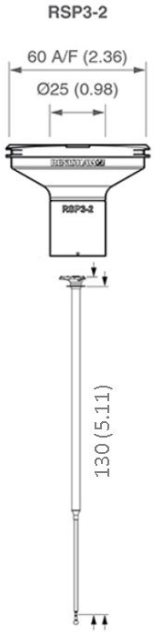

Figure 6.18: Probe dimensions, adapted from [23].

will cause a slight bending of the spring in which the effective displacement will be less than that considered. Since there is not enough information to calculate the exact value of the force that the spring exerts will be used for this calculation the value $\delta_S^{X,Y} = 0.2mm$ in order to increase the value of the force for the design factor security issues.

Since the force that a spring exerts, F_S, can be given by:

$$F_S = k \cdot \delta_S^{X,Y} \tag{6.4}$$

With k being the spring rate. F_S for a maximum displacement in the X or Y direction has the value of $F_S = 0,6 \cdot 0,2 = 0,12N$, which translates to a residual force exerted by the probe of:

$$F_C = \frac{F_S \cdot R}{L} = \frac{0,12 \cdot 12,5}{130} = 0,01N \tag{6.5}$$

This value for F_C is so residual that it will not be considered for further considerations. However, F_C associated with a displacement of the probe in the Z direction must be considered even though during the measurement, the tip exerts a force only in the X and Y direction. The probe may collide with the nozzle during the operation due to some alignment failure. If an accident occurs, the nozzle must be kept fixed so that it is possible to correct the error on the spot without having to change the position of the nozzles on the tool.

The possible collision will dislocate the probe in the positive sense. The maximum range associated to this movement is $1,7mm$. For this force balance $F_C = F_S$, as seen in 6.17. Considering the same k, it comes $F_S = F_C = k \cdot \delta_S^Z = 0,6 \cdot 1,7 \simeq 1N$.

Considering the calculation for the maximum external force that can occur in the nozzle during measurement, will be taken to account a security factor $F.S. = 2$ which translates into a permissible force of $F = F_S \cdot F.S. = 1 \cdot 2 = 2N$.

6.4.2.2 Hold-down Pressures

Since the workpiece is a revolved part, for this calculation it will be used a cylindrical coordinate system with θrz coordinates. As seen later, the maximum external force that can occur in the nozzle during measurement can assume a value of $2N$. Taking to account this residual value, it will be seen if the force of friction provident from the contact between the workpiece and the tool is sufficient to "hold-down" the nozzle.

For this application it will be considered a static coefficient of friction since the point here is to guarantee that the nozzle does not start moving. Knowing that the contact will occur between aluminum 7075 and nickel alloy steel, it will be considered a static coefficient of friction, μ_s, between aluminum and steel of $\mu_s = 0,61$ [24]. The considerable weight of the workpiece can generate a considerable force of friction. Measured with a balance, the nozzle weighs $m = 1,010kg$ and considering a gravitational acceleration $a = 9,8m/s^2$, results in a gravitational force of $F_g = a \cdot m = 1,01 \cdot 9,8 = 9,9N$. Since the workpiece is seated on a horizontal surface, normal force F_N has the same value and opposite sense of F_g.

Knowing that, the frictional force F_a is calculated by:

$$F_a = F_N \cdot \mu_s \tag{6.6}$$

Results in a F_a of:

$$F_a = 9,9 \cdot 0,61 = 6N \tag{6.7}$$

Given this value is possible to conclude that frictional forces coming from the weight are sufficient to guarantee the static condition while operating.

However, it has to be considered two mandatory factors that make the ball plungers indispensable. This fastening system needs to ensure:

- the gap between nozzles (observed in the nozzle set mount configuration mentioned in 6.4.1);
- the same position of the workpiece at any operation.

To guarantee a precision positioning and repeatability it will be followed the 3-2-1 principle based in the capacity of the ball plungers to move the workpiece.

Without any clamping system, it would be inconceivable to guarantee full contact of the nozzle surface with the tool for each operation. For this reason, the sum of the forces exerted by the ball plunger, $\sum F_{BP}$, must certify that they can dislocate the nozzle against any frictional forces. This condition guarantee that independently of the way that the

operator mounts the nozzle in the fixture, when the operator drops the workpiece, the ball plungers can move it to the same position in each operation.

Since the forces will act parallel to the same plane - $r\theta$ - to verify the previous condition, the following equation must be established:

$$\sum F_{BP} > F_a \tag{6.8}$$

As seen later the existent frictional force F_a caused by the weight has the value of $6N$.

Evaluating empirically the spring characteristics presented in Table 6.3, it will be analyzed the possibility of using the spring of $D = M4$. In the limit condition of operation of $F_{BP} = F_a$, it will be considered the minimum possible force exerted by this plunger. These design decisions are made to be on the side of safety to condition checking.

For minimum force of $F_{BP} = F1 = 4N$, seen in 6.3, can be established the force balance in plane Zr represented in Figure 6.19.

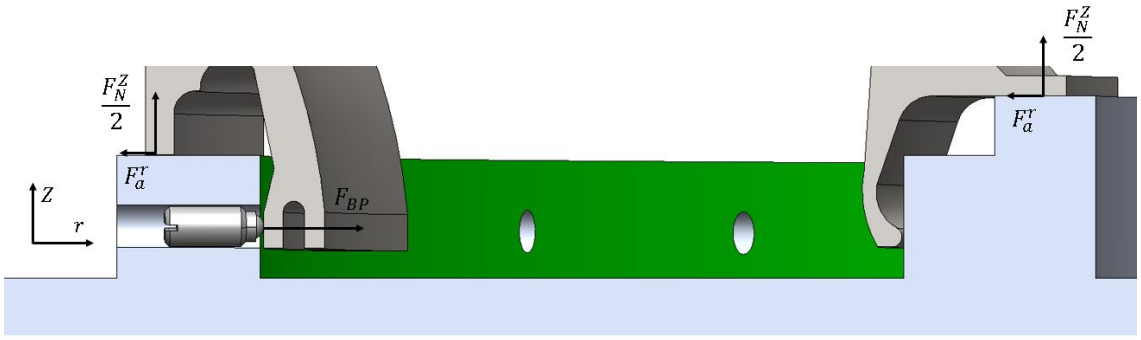

Figure 6.19: Force diagram of the fixture tool in plane Zr.

Since $F_{BP} = F1 = 4N$ and $F_a = 6N$, and to ensure that the nozzle is firmly seated it's going to be considered two ball plungers for pulling each nozzle. Keeping this in mind, the following condition must be verified:

$$\sum F_{BP} = 2 \cdot F1 = 8N > F_a \tag{6.9}$$

This means two M4 ball plungers must move the nozzle against the guide. This condition is verified to the minimum force applied by the plunger when the spring presents practically non-deformation, which will never be the real value of force since it will always be a deformation of the spring when the nozzle is in operating condition. The spring for this ball plunger as a range H of 0,8 mm, seen in 6.3. This deformation permits to exist a clearance between the guided surfaces of the nozzle and the tool's guides, which will be compensated with the ball movement in the r direction. In order to define the distance between guides for the condition that there is practically no clearance between parts, it was manufactured using AM, a prototype of the fixture tool. Since this technology has rapid and cheap manufacture, it will permit the confirmation of dimensional tolerances and verify some operational issues.

First, it was designed and printed a prototype with a distance between guides equal to the distance between the guided surfaces of the nozzle, verified in Figure A.3, of 62.9 mm. For this attempt the nozzle did not fit between guides surfaces. It was verified that for this attempt, despite in the CAD model the distance between guided surfaces was 62.9 mm, the prototype had 62,38 mm (measured with a vernier caliper). This discrepancy of values from the CAD model to the physical model is related to the difficulty in ensuring tight tolerances in AM processes due to the material expansion.

For the second attempt, it was settled in the model a distance of 63,4 mm, considering a material expansion of the same amount verified in the first attempt. In Figures 6.20 is possible to notice that there is practically no clearance in fitting and is possible to move the nozzle through the guides by hand. The distance in the prototype measured with the vernier caliper is 62,95 mm.

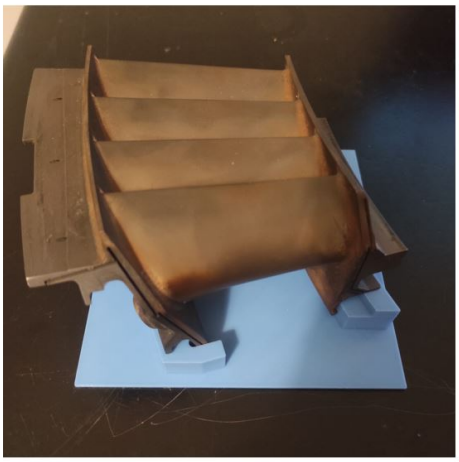

(a) Stopper clearances.

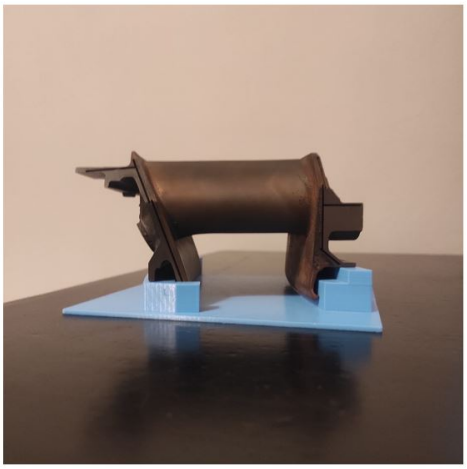

(b) Seating surfaces clearences.

Figure 6.20: Prototype visual analysis.

As seen later, is necessary to add a distance to the 62,95 mm to establish a clearance that conjugates with the spring deformation of the ball plungers. Since the ball plungers are adjustable (increasing or reducing the depth by advancing or receding the thread) and considering that for the minimal forces applied, the condition of static kinematics analysis is confirmed.

Considering a clearance equivalent to the medium value of deformation:

$$\frac{H}{2} = \frac{0,8}{2} = 0,4mm \tag{6.10}$$

If the ball plunger is adjusted so that the tip of the ball is distanced by 0,8 mm, the clearance of 0,4 mm will translate into a linear spring deformation of $x = 0,8 - 0,4 = 0,4mm$. These distances are schematized in Figure 6.21.

For manufacturing purposes, it was defined a coaxiality geometric tolerance of 0,2 mm between the two guide surfaces in order to guarantee a clearance that permits the

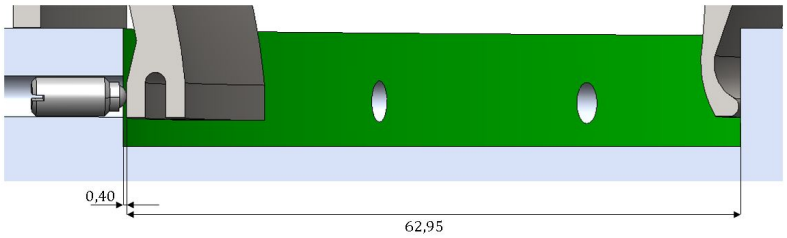

Figure 6.21: Distances, in mm, between surfaces in operational condition.

contraction of the spring. In the maximum material condition the clearance will be 0,2 mm and for the minimum material condition the clearance will be 0,6 mm. This tolerance is represented in the technical drawing present in Appendix.

In order to calculate the force F_{BP}, exerted by the ball plunger, this force can be defined by the Hook's law. This law is represented through an equation that relates the needed force to compress a spring, with a constant factor characteristic of the spring k, and a deformation x in a linear scale:

$$F_{BP} = k \cdot x \tag{6.11}$$

Since, from the table of spring characteristics there is no access to the spring rate but knowing from Hooks law that F_{BP} has a linear relation with x, is possible to calculate F_{BP} for $x = 0,4mm$. Using linear interpolation with the values $F_{BP}(x = 0mm) = 4N$ and $F_{BP}(x = 0,8mm) = 10N$, it comes:

$$\frac{F_{BP}(x = 0,4mm) - 4}{0,4 - 0} = \frac{10 - 4}{0,8 - 0} \Leftrightarrow F_{BP}(x = 0,4mm) = \frac{10 - 4}{(0,8 - 0)(0,4)} + 4 = 7N \tag{6.12}$$

It means that for the configuration assumed above one ball plunger exerts a force of $7N$ in the operating condition.

The last consideration is the calculus of the sum of the forces that contribute to hold down the workpiece. The forces that ensure the fixture of the tool are the frictional forces coming from the weight and the ball plungers. The F_a calculated before acts in any movement occurring parallel to the $r\theta$ plane, i.e., only contributing to holding the workpiece in the r and θ direction. The force of friction from the ball plungers contributes to holding the workpiece in all directions r, θ, and z. The force diagram representing the acting forces coming from the ball plungers is represented in Figure 6.22.

The forces balance in plane $r\theta$ is represented in Figure 6.22.

From the force diagram above is possible to establish an equation that relate that forces acting in the radial direction r and in θ:

$$2 \cdot F_{BP} = F_N^r \leftrightarrow F_N^r = 2 \cdot 7 = 14N \tag{6.13}$$

Where:

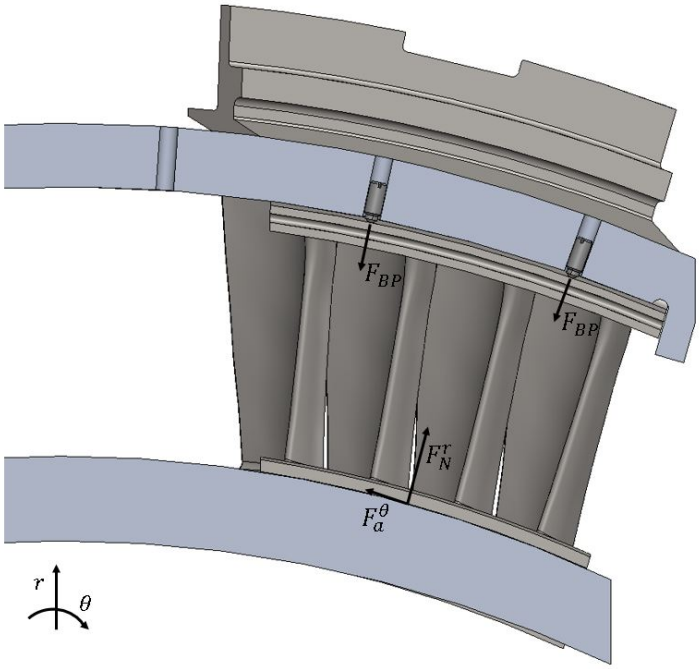

Figure 6.22: Force diagram of the fixture tool in plane $r\theta$.

$$F_a^\theta = F_N^r \cdot \mu_s = 14 \cdot 0,61 = 8,54N \tag{6.14}$$

The hold down forces exerted in one nozzle in $r\theta$ are represented in Table 6.4.

Table 6.4: Force results from friction and the ball plungers.

Directions	Ball plunger	Friction
r	14 N	6 N
θ	0 N	14,54 N

From this table is possible to conclude that in r direction, the force exerted by the ball plungers can move the workpiece against the frictional force. It also can be observed that in θ direction, the operator when sliding the nozzle has to overcome the frictional force of 14,54 N.

The final design of this tool is represented in a technical drawing present in the Appendix. Apart from the geometric tolerance of coaxiality, associated to the guide surfaces, is also defined a parallel geometric tolerance between the seating surfaces and the surface in contact with the granite bed. This tolerance is defined to guarantee the parallelism between workpiece surfaces oriented in plane $r\theta$ and plane xy of the CMM. After contact with the machining section TMA's, it was established a value of 0,02mm for this tolerance taking to account the CNC milling manufacturing limitations.

7

LPT Nozzle Exit Flow Area Dimensional Inspection

The dimensional inspection of exit flow areas of nozzles can be performed in different ways. For example, it can be used a measuring instrument dedicated to this type of inspection. Or use a more versatile device that allows the measurement of various geometries and capacities this instrument to inspect. Regarding the route to be adopted, it is necessary to take into account several factors such as: whether there is already some dedicated equipment or whether this instrument will have to be developed; the cost and difficulty of creating a new tool or enabling equipment to perform this inspection; and the accuracy of the measurement of these two possible ways of inspecting.

As seen previously, TAP has a CMM with very high measurement accuracy, allowing for measurement programs. The creation of the measurement program for the LPT nozzle of the CFM56-5B will be the last approach of this thesis that will have in view a future application and inclusion of the program in the inspection performed at TAP to these engines.

The process of obtaining the exit flow area value is an extensive one that is divided into several steps:

- Developing a parametric model of the nozzle;
- Securing the nozzle in a specific position on the machine;
- Defining the location of the area to be measured;
- Running an automated program on the CMM.

As seen in the previous chapters the model and the clamping tool are already developed, so it is necessary to define the exact location of the area to be measured.

A prototype of the clamping tool was used for the measurement at TAP. Due to priority constraints, it was not possible to manufacture the clamping device. Being aware of the current capacity situation of the workshop throughout the study, the study of the clamping tool was not deepened in terms of manufacturing. The project and the drawings presented can be seen as the suggested tool considering geometric and dimensional tolerancing conditions and not believing the tools and manufacturing processes used to

produce the fastener tool. Thus, it would be interesting in future work to deepen the study in terms of manufacturing to execute this tool's production.

As stated in Chapter 3, the reason for this study is primarily focused on the influence these areas can have on engine performance. In this work, the measurement procedure was only developed for one nozzle, i.e., the measurement program only serves to inspect one nozzle at a time. Therefore, the ideal inspection procedure would be to establish a measurement program that examines all areas of a set at once. As a future development, the ideal would be to place the group of LPT nozzles mounted on the granite plane, measure all areas and generate a report with the distribution of results over the set. In this way it would be possible to relate the distribution of the different areas by set with the engine performance on the test bench.

7.1 Location of the exit flow area

The area calculation is done after the acquisition of a closed contour by the CMM. The closed contour is defined by several points. These points are connected by line elements in order to define a closed contour. The points are obtained by traversing the section that has to be defined in the program.

This study incorporates, in addition to the development of a product, an analysis and investigation of the location of areas for the flow of this type of parts. However, there is a perception of the place of the areas present in studies seen in a previous chapter. The section that defines the exit flow area is the manufacturer's property that is unavailable. In this case, even the companies responsible for the repair and inspection of this type of parts have access to this information. Thus, it is TAP's interest to invest in this study to be able to perform this type of inspection in the future. The possibility of carrying out this process is internally, allowing for high efficiency in terms of management since to carry out this type of measurement the part has to be transported abroad (to entities capable of carrying out this operation). Also allows for a reduction in associated costs, since the machine will be capable to inspect without additional costs.

Although there is a perception of the location of the areas present in studies seen in a previous chapter, after analyzing the CFM documents available, there is no engine manual that refers to the location and position of the section that defines the exit flow area. However, reference is made to these areas, assigning ranges of allowable values, demonstrating the importance they may have for the manufacturer.

In order to begin this study, two LPT nozzles from the CFM56-5B engine were shipped overseas to be measured the exit flow areas. These two nozzles used were inoperable parts that were in the scrapyard due to corrosion problems related to the coating. These non-conformities do not in any way affect the possibility of considerable deformations in the trailing edges that could tamper with the exit flow area values. However, it will be considered that these parts have already had several cycles of operation and show wear like any other. One of the parts that were sent was the one used to make the CAD model

(reference nozzle), and the other (secondary nozzle) serves only to increase the sample of values, increasing the credibility of the investigation process. The reports can be found in the Annex I.1 and I.2. In order to be able to analyze exit flow areas for the secondary nozzle, it was realized a scan before the two nozzles were sent abroad to be able to work on the two models while waiting for the results from the manufacturer.

As seen previously and can be seen in the appendixes A.1 and A.2 the CAD model of the reference nozzle has a high accuracy compared to the mesh from the scan. This way it will be used this model in SolidWorks to obtain area values and compare them with the report values. For the reference nozzle, SolidWorks will also be used for calculation, however, it will be worked directly on the mesh since the process of developing the CAD model is quite time-consuming and not justifiable for this study.

SolidWorks mesh processing is limited. The presence of meshes with more than 10000 nodes makes the program unable to process. In order to ensure maximum accuracy in the area without compromising the processing by SolidWorks, a mesh optimization was performed using MeshLab. This program allows you to apply filters to clean the mesh and work the mesh by zones. This allows a very refined mesh to exist in the area of the vane and to decrease the quality of the mesh, for example, in the platform zone. That will ensure that values obtained have a reasonably high accuracy without problems related to SolidWorks processing. The mesh optimization is represented in Figure 7.1.

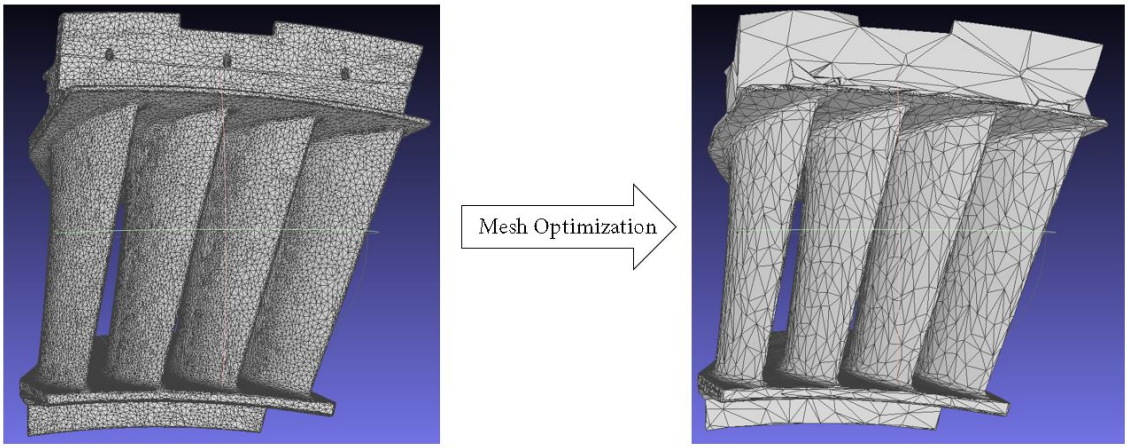

Figure 7.1: Mesh optimization.

7.1.1 Method to Obtain Exit Flow Area Values with SolidWorks

The method for obtaining values for the areas in SolidWorks always involves the following steps: draw a centerline coincident with the trailing edge, generate a plane perpendicular to this centerline, perform a section view of this plane, draw the line that will define the section corresponding to the exit flow area, generate the plane overlapped with this section, perform a slicing of this plane with the model, obtain a closed contour referring

to the flow, use the "section properties"command to obtain the value of the area. This process is represented in Figure 7.2.

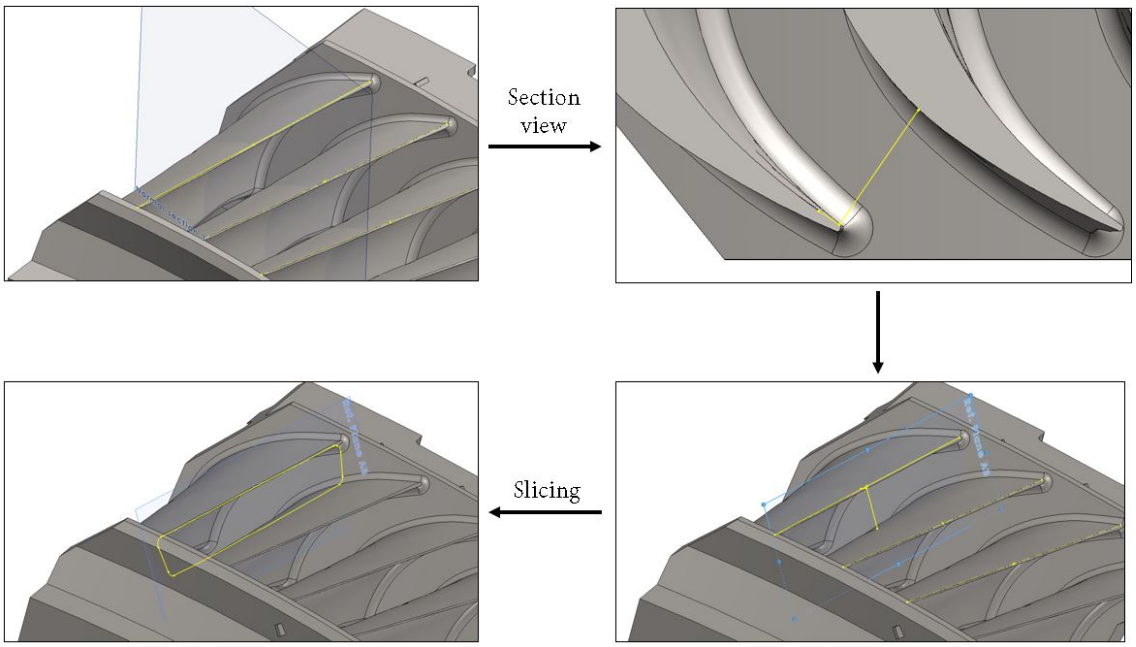

Figure 7.2: Process to obtain a contour for the flow area.

7.1.2 First Approach

The bibliography consulted refers to the location of the exit flow area as a section perpendicular to the flow located near the trailing edge. Thus, and as a first approach, it was considered the trailing edge of each vane as the reference. To obtain a considerable sample of values to be compared with the result of the report, a strategy related to an iterative process was defined: 5 planes perpendicular to the pressure surface of the vane with a distance of 0.5 mm to a depth of 3 mm from the trailing edge were defined. After generating the slicing between those planes and the model the resultant sketches are represented in Figure 7.3. It will be considered for now on the numeration of the sections represented in 7.3.

With this strategy applied to the reference nozzle and following the method of obtaining values described above it is possible to outline a sample of results that is represented in the following table.

From these results is possible to notice that for the three sections, the area values remain approximately the same. The values seen in the report I.1 present an oscillation. The measured exit flow area from section 1 is considerable superior comparing to section 2 and section 3, that pattern is not seen in the sample obtained. Even considering the difference of values obtained in SolidWorks and in the CMM, the sample presents a

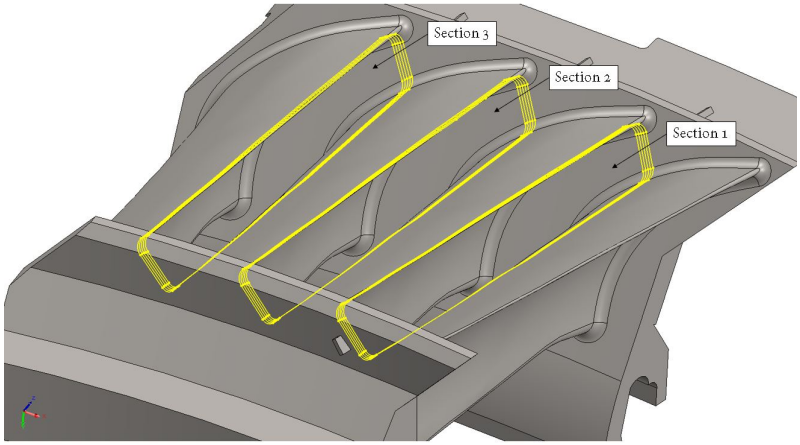

Figure 7.3: Contour sketches obtained from the first approach.

Table 7.1: First approach sample

Sample	Section 1 $[mm^2]$	Section 2 $[mm^2]$	Section 3 $[mm^2]$
1	881,583	882,159	882,568
2	886,292	887,028	887,403
3	891,441	892,239	892,678
4	897,025	897,936	898,393
5	903,012	904,073	904,515
Report	855,999	852,571	852,422

considerable deviation. All these facts takes to conclude that this approach seems to have an error.

7.1.3 Second Approach

In this second approach the engine shaft axis was considered as a reference. This approach in relation to the previous includes a consideration that must be taken into account. In case there is deformation associated with the trailing edges (due to deterioration of operation), when the first approach is considered, the section will be dislocated with the possible displacement that the trailing edge has undergone. This leads to the area values all being quite identical since for each measurement their reference is changed.

Knowing that each set of LPT nozzles consists of 24 nozzles and taking into account that each nozzle has 4 vanes it is possible to define the existing α angle between vanes in relation to the engine shaft axis:

$$\alpha = \frac{360}{24 \cdot 4} = 3{,}75^\circ \tag{7.1}$$

Taking to mind the angle between planes that define sections, is necessary to establish a first section, so it's possible to generate the planes rotated by 3,75 degrees with respect to the shaft axis, represented in Figure 7.4. The first section was obtained by creating a

plane defined by the line between the trailing edge of one vane and the nearest possible point of the next vane.

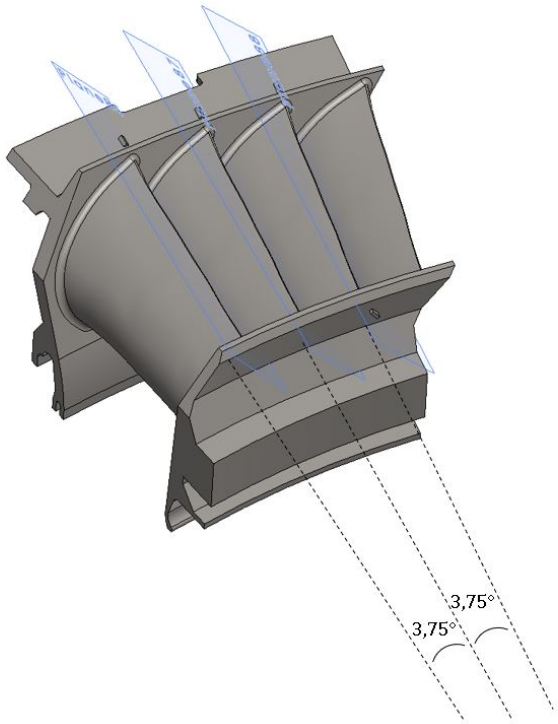

Figure 7.4: Planes that define sections.

Applying the method to obtain area values with SolidWorks to the reference nozzle, is possible to obtain a sample of results that is represented in Table 7.2.The sample 1 is obtained defining the section 1 as the first section, and generating section 2 and section 3 by a circular pattern. The sample 2 is obtained defining the section 2 as the first section, and generating the section 1 and section 3 by a circular pattern, and the sample 3 is obtained defining the section 3 as the first section, and generating section 1 and section 2 by a circular pattern.

Table 7.2: Second approach sample for the reference nozzle.

Sample	Section 1 $[mm^2]$	Section 2 $[mm^2]$	Section 3 $[mm^2]$
1	879,685	878,587	877,669
2	879,465	876,998	876,132
3	881,142	878,973	877,213
Report	855,999	852,571	852,422

Although the are values obtained are much higher than those in the report, the values present a concordant pattern with the report. From the values seen in the report I.1, is noticeable that section 1 is greater than section 2 and section 3. Is perceptible that section 2 and section 3 present similar values of exit flow area which is observed in the samples too.

In order to conclude which sections are suitable to be defined as those to be measured in the CMM, the deviation calculations were made and are presented in the Table 7.3. In this Table is compared the values obtained in SolidWorks with the report values. Deviation 1 corresponds to the difference between Sample 1 and Report values, Deviation 2 corresponds to the difference between Sample 2 and Report values, and so on. Since it is considered in the report the sum of the section values, it will be considered this parameter too.

Table 7.3: Second approach sample deviations for reference nozzle (values in mm^2).

Section	Report	Sample 1	Dev. 1	Sample 2	Dev. 2	Sample 3	Dev. 3
Section 1	856,00	879,69	23,69	879,46	23,46	881,14	25,14
Section 2	852,57	878,59	26,02	877,00	24,43	878,97	26,40
Section 3	852,42	877,67	25,25	876,13	23,71	877,21	24,79
Sum	2560,99	2635,95	74,96	2632,59	71,60	2637,32	76,33

Analyzing the results, is possible to conclude that the sample with the lowest error associated to the sum of all sections is the Sample 2. The sum of the sections is a parameter considered in the report, so it will be the decisive factor to choose the workable sample.

With this method applied for the secondary nozzle and following the method of obtaining area values is possible to outline a sample of results that is represented in Table 7.4.

Table 7.4: Second approach sample for the secondary nozzle.

Sample	Section 1 [mm^2]	Section 2 [mm^2]	Section 3 [mm^2]
1	869,023	855,234	844,502
2	861,296	850,621	844,371
3	865,409	852,955	845,576
Report	865,053	842,990	833,899

From these results is possible to notice that for the three sections, the area values present a concordant pattern with the report. The values seen in the report I.2 present a declining, the measured exit flow areas are decreasing from section 1 to section 3 which happens in the sample obtained. In order to conclude which sections are suitable to be defined as those to be measured in the CMM, the deviation calculations were made and are presented in the Table 7.5.

Table 7.5 represents the comparison between values from SolidWorks with the values from the report obtained in CMM. Analyzing the results, is possible to conclude that the sample with the lowest error associated to the sum of all sections is the Sample 2. An cumulative error of $14,3mm^2$ in 3 measured values, considering a tolerance defined in the report of $50,34mm^2$, is a positive starting point. This same analysis for the reference nozzle, leads to the sample 2 to be the workable sample. Taking to account the amount of parameters involved and the absence of any reference to the position of this section in the

Table 7.5: Second approach sample deviations for secondary nozzle (values in mm^2).

Section	Report	Sample 1	Dev. 1	Sample 2	Dev. 2	Sample 3	Dev. 3
Section 1	865,05	869,02	3,97	861,30	3,75	865,40	0,35
Section 2	842,99	855,23	12,24	850,62	7,63	852,95	9,96
Section 3	833,89	844,50	10,60	844,37	10,47	845,57	11,67
Sum	2541,9	2568,7	26,8	2556,2	14,3	2563,9	21,9

engine manual, the Sample 2 presents a considerable precision. In conclusion, the sections that define the exit flow area, which will be used to perform the CMM measurement, are those defined by Sample 2. That is, the sections obtained by defining the section 2 first, and generating section 1 and section 3 by the circular pattern of 3,75 degrees.

7.2 CMM program

CMM is used by TMA's every day to inspect countless parts dimensionally. It is widespread to use this equipment to measure the diameters of various parts. The CMM has very high accuracy and can obtain values reasonably quickly. For example, using the joystick, through three points, it is possible to obtain a value for the diameter and circularity of this circle, which validates the result obtained.

Currently, some measurement programs have already been developed to perform dimensional inspections of non-prismatic parts, which would be impossible to obtain operational results using only the manual movement of the tip. The work developed by colleagues Rendas P. and Farinha E. allowed, together with the TMA's, to facilitate the development of the measuring program for fan blades, which is currently used daily in the workshop, in production proportions.

Although a CMM program for flow area measurements has never been performed, nor is there any model available that would be useful to perform this program, the TMA's knowledge and experience in developing dimensional inspection programs in CMM were crucial to perform this work.

7.2.1 Set-up and Alignment

The orientation of the nozzle on the granite plane of the CMM greatly influences the measurement process's efficiency. As seen previously in Chapter 6, the arrangement of the nozzle on the CMM will be with the trailing edge pointing upwards, i.e., in the positive direction of the Z-axis. The development of clamping tool for this configuration was developed in Chapter 6. However, the fabrication of this tool is a time-consuming process that was not accomplished in time to perform the tests on the CMM. Thus, a program will be carried out to test and confirm the work developed. For this test, only one nozzle will be used, indicating that only the three directly available areas will be measured; in this way, it is possible to use the prototype printed using AM. The prototype

mainly ensures that the seating surfaces on the HPT shroud are parallel to the granite plane as if the nozzle had been mounted on the set.

The prototype was used as part of the set-up, yet the prototype is in no way blocked from the granite plane. The only force that acts is the frictional force, which in the end, is not enough to prevent any movement. This way, prismatic boulders, which have a high mass and can block the prototype, can be seen in Figure 7.5. The prismatic geometry of these jigs also allows them to be oriented according to the machine's referential, defining a first part 0 and greatly facilitating the pre-alignment. The referential of the pre-alignment and the 0 pieces can also be seen in Figure 7.5.

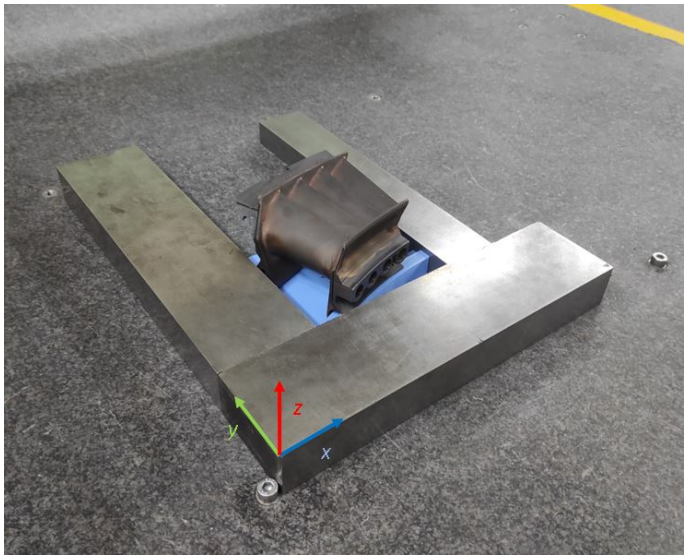

Figure 7.5: Provisional set-up.

With this setup in place, it defines the pre-alignment. In Figure 7.6 you can see the creation of the pre-alignment referential represented also in Figure 7.5. The view represented in Figure 7.6 corresponds to the XY plane. Note that the blue vertical line corresponds to the YZ plane and the horizontal line to the XZ, the blue rectangle corresponds to the XY plane, and the green cross corresponds to the referential's origin. Note also that the red circle indicates the position of the tip in real time and that, in this case, it was in contact with the origin of the CAD model referential that is represented in Figure 7.7.

As can be seen, the YZ plane of the cad model is not parallel to the referential defined in the CMM. The plane is rotated in relation to the z-axis. In order to define a more precise pre-alignment, the existing angle between the YZ planes of the model and the CMM was calculated. Having already saved in the program the YZ plane of the CMM, it is necessary to define in MCOSMOS the YZ plane of the model. This is done by obtaining at least 3 points that are capable of generating a plan. It was concluded that the referential plane presents an angle of approximately 90 degrees while the model plane presents an angle of 73.8 degrees. After completing this operation, the physical model of the part is already pre-aligned with the digital model stored in MCOSMOS, and it is already

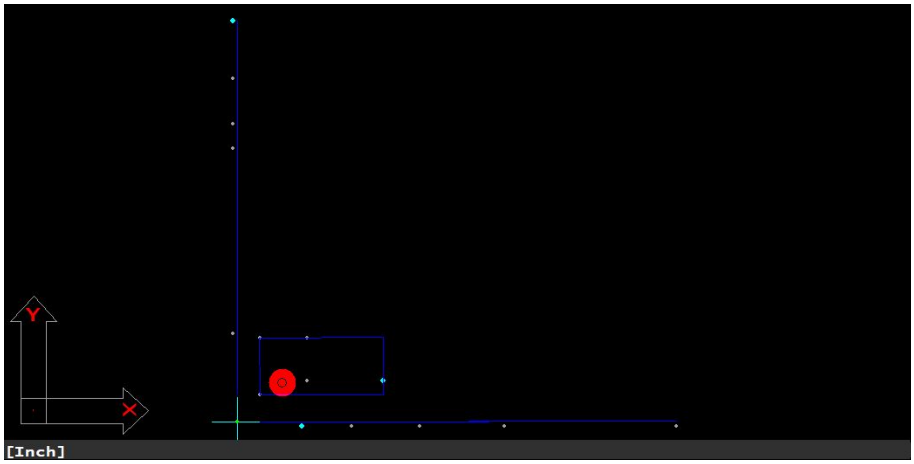

Figure 7.6: Pre-aligment.

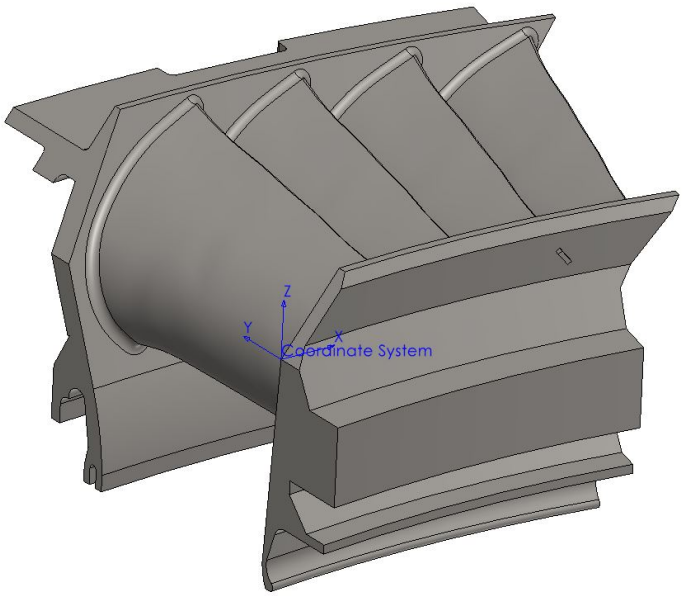

Figure 7.7: CAD Model Coordinate System.

possible to calibrate the probe to a position, of $\beta = 75°$ and $\theta = 45°$,in order to be able to measure all areas with the probe fixed in one position. The calibration process is done whenever a new position needs to be added for the RSP3-2 probe and consists of clamping a calibration ball to the granite table, which can be seen in Figure 7.8. The program runs automatically.

After setting the pre-alignment in MCOSMOS, it is necessary to set the clearance height. This height represents the plane from which the probe can move with maximum speed, i.e., it ensures that the program execution is the fastest and that no abrupt collision will occur. The plane defined by the clearance height is shown in Figure 7.9.

With what is already defined, it is possible to move on to programming the movements that will be part of the measurement process. With the pre-alignment already established,

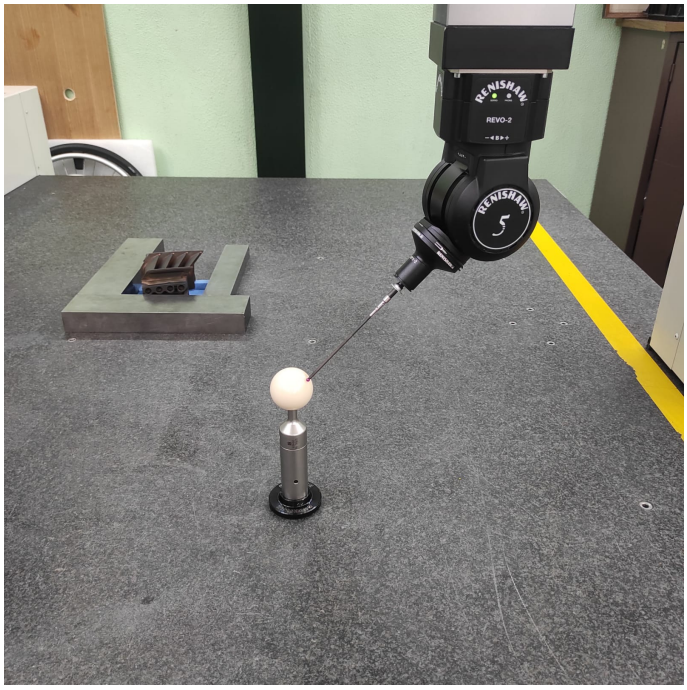

Figure 7.8: Calibration to position $\beta = 75°$ and $\theta = 45°$.

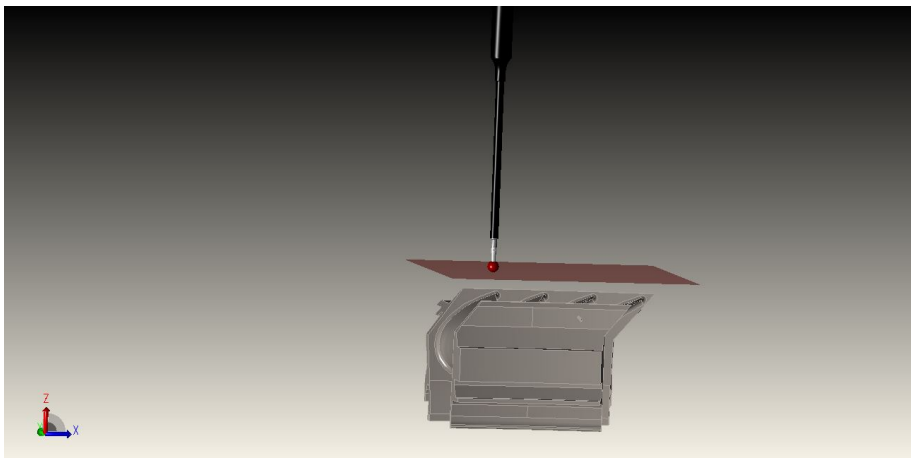

Figure 7.9: Clearance height.

it is possible to define the alignment that will be used.

When the nozzle is positioned in the CMM, the program has no record of the exact position of the part. In short, alignment consists of matching the physical model with the CAD model in MCOSMOS. In CAT1000PS, there are two types of alignments that can be used: Reference Point System (RPS) e best-fit. RPS consists of acquiring 3-2-1 points from the physic model and comparing them to their nominal placement in space from the CAD file. Six measure points from the sub-part are used to generate a referential, which is then compared to the nominal one formed with the model's points [25]. The best fit consists in iterations that turn and rotate the points so that the deviations as a whole get minimized. The program has the option to choose the maximum number of iterations and the deviation target. This means that the software will read 6 points (strategically chosen

by the operator) on the first iteration and calculate the first deviation. If the deviation value is superior to the target, the software proceeds to the second iteration. If the target is not achieved after a defined maximum number of iterations, the program does not advance. For this program, it was defined by six iterations to a target of 0,005 inches. Six points are sufficient to block the movement of the workpiece by the 3-2-1 principle seen before. The same principle defines the alignment, and the disposition of the six points is represented in Figure 7.11.

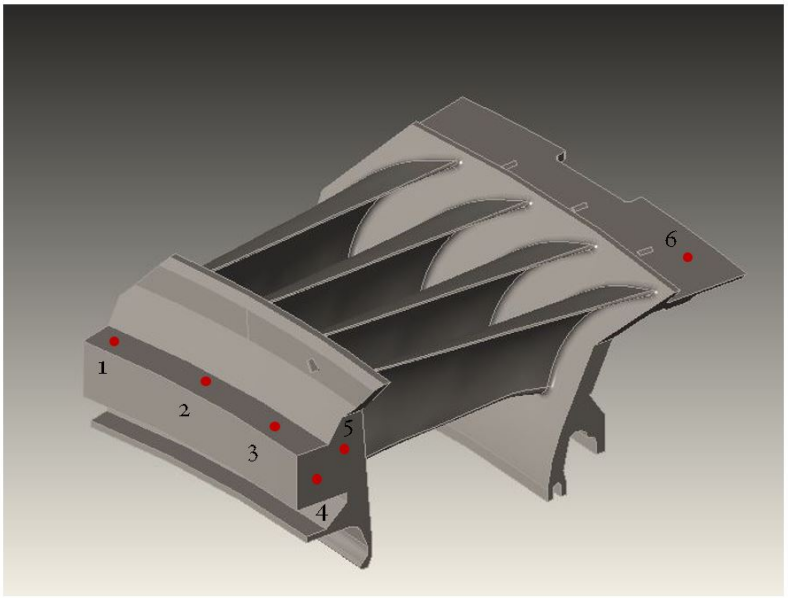

Figure 7.10: Six points defined for best-fit alignment.

To notice that the location of these points were chosen strategically on planar surfaces which are perpendicular to each other to facilitate the calculation process. The alignment commands are represented in Figure A.6. After three iterations the maximum deviation detected was 0,034 inches, lower than the target delineated.

7.2.2 Exit Flow Area Section Scanning

With the CAD and physical models aligned, it is possible to determine the sections to be measured and the type of scan to use. After the CNC mode is turned ON, it is possible to define the sections due to CAT1000PS command "Create a section with cutting plane". In order to be able to create the sections defined in 7.1.3, three artifacts were created in the CAD model whose faces coincide with the cutting plane that defines the section to be measured. When the face of the artifact is selected, the CAT1000PS command cuts the model and enhances all the visible contours in that section. The artifacts surfaces and the slicing sketch is represented in Figure 7.11.

Using the command "Redefine section" it is possible to select the contour that defines the exit flow area. The Scan CNC menu and the contours for section 1 and section 2 are represented in Figure 7.12. In this menu is possible to choose where the probe starts and

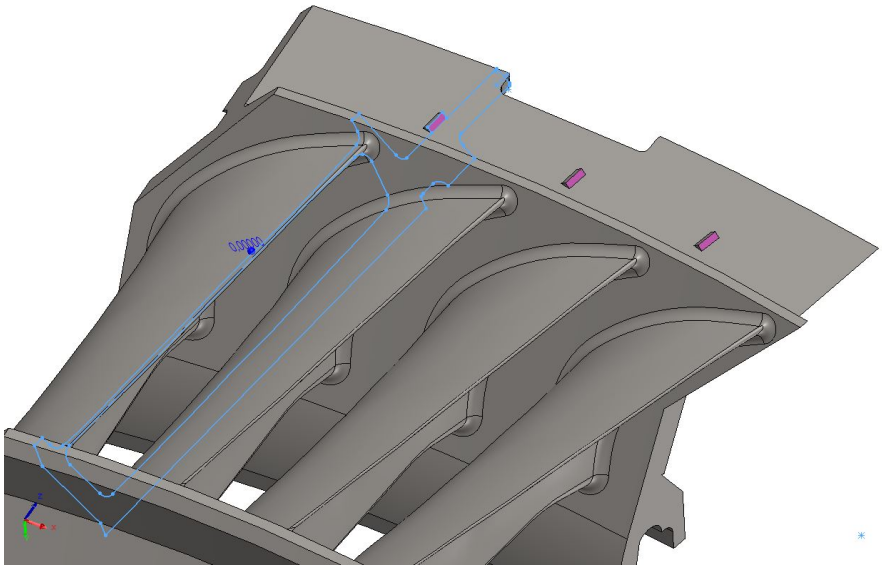

Figure 7.11: Artifact surfaces to define a section.

ends the scan, the name of the section, the scan speed, and the pitch. The pitch is defined by the rate acquisition of points, i.e., defining a pitch of 0.05 inches, the machine will generate points every 0.05 inches traveled that will define the contour. The lower the pitch, the higher the contour accuracy, but the lower the machine's processing speed.

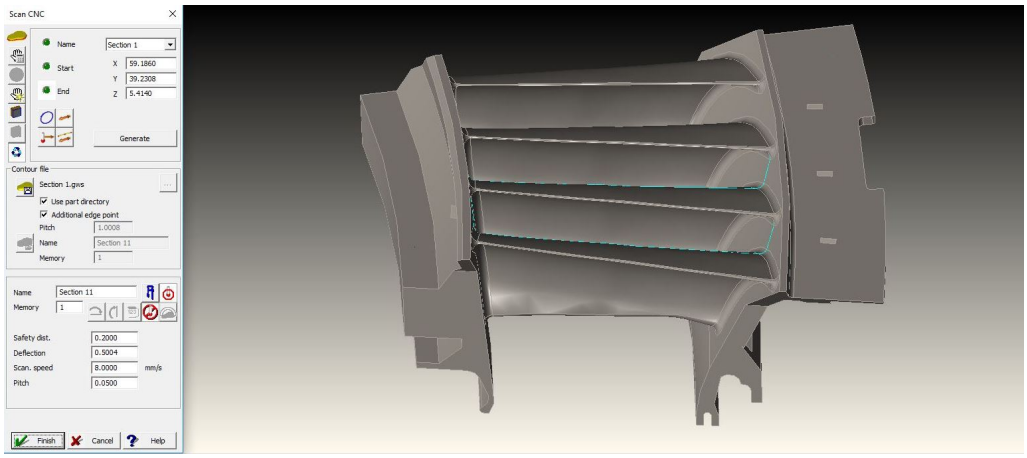

Figure 7.12: Scan CNC mode.

With all the input described above is possible to proceed to the scan. In this first approach it will be measured a section at a time. After the tip has traveled the perimeter that defines Section 1 it was generated a contour (represented in green) that is represented in Figure 7.13. Is possible to observe from this 3D perspective the angle correspondent to the rotation in the pre-alignment represented in green, the planes in blue defined in pre-alignment and the origin of the CAD model.

Analyzing the zoomed in view of the contour is possible to notice that the radius of the fillet are lucid, i.e. the software was capable to acquire sufficient points in that area

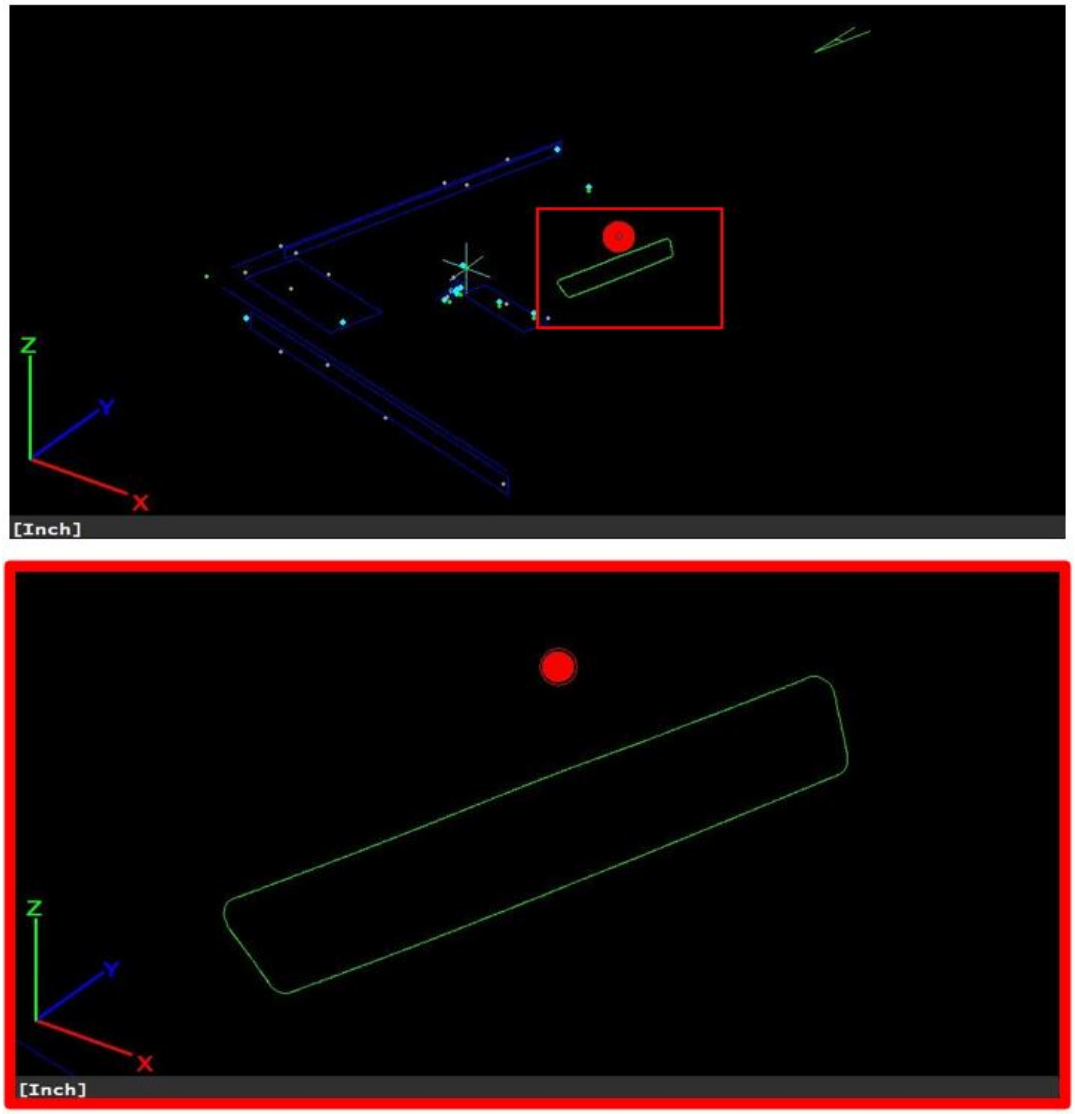

Figure 7.13: First area contour.

in order to form a clear curvature.

7.2.3 Area Calculation and Results

The area calculus command "CntrArea" in MCOSMOS only calculates projected areas based in the Gauss area formula.

This formula permits the calculus of complex polygon's areas. For a polygon defined by a counter clock wise sequence of points $P_i = (x_i, y_i)$, with $i = 1, ..., n$, the area A of the closed contour defined by P_i is:

$$A = \frac{1}{2} \sum_{n}^{i=1} (y_i + y_{i+1})(x_i - x_{i+1}) \tag{7.2}$$

Being n the number of points that constitute the contour and, since the scan is done

in a counter clock wise direction and generate points sequentially, this formula can be applied to calcute the area.

Since this contour is a two-dimensional geometry in a three-dimensional orientation, if the area calculus command was applied directly, the software would return the XY projected area. To obtain an area value for 3D contours it is necessary to, st first, generate a coincident plane with the contour section. This plane is obtained automatically by retaining 3 points that constitute the contour, represented in steps 20, 21 and 22 of Figure A.5. In the next step is done the alignment with the plane defined and then applied the "CntrArea" command to calculate the area of the closed contour projected on the defined plane.

The results for the exit flow area calculated by MCOSMOS are resumed in Table 7.6.

Table 7.6: Exit flow area results measured by CMM.

Section 1 $[mm^2]$	Section 2 $[mm^2]$	Section 3 $[mm^2]$
868,837	869,353	869,031

8

Conclusions

This dissertation is framed in a business environment, in this case, linked to TAP M&E Engine Shop. In a general view, these works provide a symbiotic relationship between student/faculty and company. While the student, by developing his work, deepens his knowledge in a more specific engineering area, the company gains by developing projects or theoretical studies that are useful for its growth.

During this study, TAP always presented high availability of resources, so I could develop my work without constraints. I was allowed to work with the equipment practically autonomously, with only one TMA supervising. This autonomous use of the equipment allowed me to obtain experience and extensive knowledge about this type of machines related to dimensional inspection and metrology.

This study was a reverse engineering project divided into several steps starting from a scrap part and ending in a CMM program to inspect exit flow areas. Several engineering areas were covered, including mesh handling, dimensioning and tolerancing, CAD modeling, design methodologies, alignments, and CMM programming.

8.1 Final Results

In hindsight, the main objective of this study was completed. Results for exit flow area were obtained using the program developed in CMM's TAP engine shop. The results were analyzed in detail in Chapter 7, and Table 8.1 resumes all the results for the reference nozzle.

Table 8.1: Final Results

Sample	Section 1 $[mm^2]$	Section 2 $[mm^2]$	Section 3 $[mm^2]$
SolidWorks	879,465	876,998	876,132
Mitutoyo CMM	868,837	869,353	869,031
Report	855,999	852,571	852,422

From these results is possible to notice a pattern in all samples, apart from the linear difference of values between samples. The difference in area values is possibly related to

the area calculation method. The obtained contour is generated from the lines between the points found when scanning the section. Missing points in the area of the radius of curvature can lead to a decrease in the area value relative to the true section. This situation is represented in Figure 8.1.

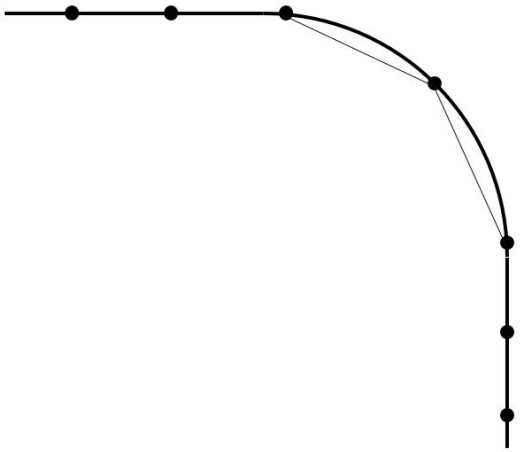

Figure 8.1: Point acquisition problem in radius of curvature zone.

In this situation, the calculated area is less than the nominal because there are small areas that are not counted for this effect.

The validity and reliability of the results can only be sustained with a larger sample of measurements. A larger sample was not possible to achieved due to some constraints such as: reconciling the development of this work with the shop production work (which is always a priority), the time it took to deliver the reports by the entity that measured the nozzles, and the complex and time-consuming processes involved in the steps before the final measurement itself.

With the program and content already developed, it will be possible to move forward in this study to validate results obtained in CMM with the manufacturer's results or even standardize this process internally by obtaining a nominal area value and allowable deviations through internal statistical process controls.

In summary, several products were designed and developed that will be useful to give continuity, not only to the theme of this dissertation in specific, but also may be convenient for the evolution of other repair/inspection processes. The following is left as developed material:

- Various meshes of LPT nozzles in STL files that can be used for measurements on the model of complex geometries, such as the radii of curvature of the leading and trailing edge;

- CAD model in STEP format that can be used to download to software's for the purpose of, for example, developing automatic repair processes that require reading a parametric model;

- A prototype and design of a fixture tool for the purpose of clamping the nozzle for dimensional inspection of the exit flow areas. The tool was designed specifically for this purpose. However, it can be used for other types of CMM measurements of dimensions specified in the manufacturer's manual that are available in the defined configuration;
- The CMM program for measuring the flow areas of a LPT nozzle, including pre-alignment and alignment. This program can be the basis for creating other programs to measure any kind of areas of other engine components.

8.2 Future Work

The work developed in this study is just the beginning of a project that may eventually be integrated into TAP engine shop production. There is still a lot of work to be done in order to certify this inspection as an integral part of the repair process.

As mentioned earlier, in this study, only one test measurement of one LPT nozzle was made using the program developed at CMM. The sample of results is insufficient to validate the results. Therefore, in the future, the goal is to first send more nozzles abroad in order to have more terms of comparison. By having more reference values from a manufacturer's certified process, it is possible to get a better approximation of the location of the flow area. In this way, the validation of results involves testing and modifying the program in order to match the area values measured abroad and those measured at the TAP for the same nozzle.

A prototype of the clamping tool was used for the measurement at TAP. Due to priority constraints, it was not possible to manufacture the fixturing tool. Being aware of the current capacity situation of the workshop throughout the study, the study of the clamping tool was not deepened in terms of manufacturing. The project and the drawings presented can be seen as the suggested tool considering geometric and dimensional tolerancing conditions and not considering the tools and manufacturing processes used to produce the fastener tool. Thus, it would be interesting in future work to deepen the study in terms of manufacturing to execute this tool's production.

As stated in Chapter 3, the reason for this study is primarily focused on the influence these areas can have on engine performance. In this work, the measurement procedure was only developed for one nozzle, i.e., the measurement program only serves to inspect one nozzle at a time. Therefore, the ideal inspection procedure would be to establish a measurement program that examines all areas of a set at once. As a future development the ideal would be to place the group of LPT nozzles mounted on the granite plane, measure all areas and generate a report with the distribution of results over the set. In this way it would be possible to relate the distribution of the different areas by set with the engine performance on the test cell.

Bibliography

[1] J. M. Lourenço. *The NOVAthesis LaTeX Template User's Manual*. NOVA University Lisbon. 2021. URL: https://github.com/joaomlourenco/novathesis/raw/master/template.pdf (cit. on p. ii).

[2] T. A. Portugal. *TAP Maintenance & Engineering*. URL: https://www.tapme.pt/ (cit. on p. 4).

[3] R. Royce. *The Jet Engine*. Fifth edition. The Technical Publications Department, 2019 (cit. on pp. 5–7, 12, 13).

[4] G. S. L. M. Spence. "The CFM56 Engine Family An International Development". In: (4 1988), pp. 1–7. DOI: 88-GT-296 (cit. on p. 7).

[5] C. A. Engines. *The CFM56 Engine*. URL: https://www.cfmaeroengines.com/engines/cfm56/ (cit. on p. 7).

[6] C. C. T. Center. *Training Manual CFM56-5B Basic Engine*. First edition. CFM International, 2000 (cit. on pp. 8–11).

[7] E. H. T. G. P. Sallee H. D. Kruckenberg. *Analysis of Turbofan Engine Performance Deterioration and Proposed Follow-on Tests*. First edition. National Aeronautics and Space Administration, 1975 (cit. on pp. 13, 14).

[8] J. G. Wilson. *The Design of High-Efficiency Turbomachinery*. Second edition. Massachusetts Institute of Technology, 2014 (cit. on p. 14).

[9] M. Meyer. "ANALYSIS OF HIGH PRESSURE TURBINE NOZZLE GUIDE VANES CONSIDERING GEOMETRIC VARIATIONS". In: (2016), pp. 1–12. DOI: GT2016-57502 (cit. on pp. 15, 16, 22, 23).

[10] M. D. Zao Ni Tsung-chow Su. "An empirically-based model for the lift coefficients of twisted airfoils with leading-edge tubercles". In: (2018), pp. 1–12. DOI: https://doi.org/10.1063/1.5023103 (cit. on p. 15).

[11] Creaform. *HandySCAN 3D | BLACK Series, Especificações Técnicas*. URL: https://www.creaform3d.com/pt/solucoes-em-metrologia/scanners-3d-portateis-handyscan-3d (cit. on pp. 17, 25).

[12] G. of Canada. *Patent 2600926 Summary*. URL: https://brevets-patents.ic.gc.ca/opic-cipo/cpd/eng/patent/2600926/summary.html (cit. on p. 17).

[13] P. Rendas. "Fixture Design and Process Development for High Pressure Compressor Rotor Blades Measuring in Aircraft Engine Maintenance". In: (2021), pp. 1–45 (cit. on pp. 20, 22, 31, 33).

[14] Mitutoyo. *Geometrical 3D-Measurement Software for Co-ordinate Measuring Machines User's Manual v4.2*. Mitutoyo, 2019 (cit. on p. 20).

[15] J. Graefe. *MCOSMOS v3.1 Setup I++*. Mitutoyo, 2013 (cit. on p. 20).

[16] E. Farinha. "Fixture Design and CMM Program Development for Measuring of High Pressure Compressor Rotor Blades". In: (2022), pp. 1–175 (cit. on pp. 22, 31).

[17] F. Baptista. "A 0-D Off-Design Performance Prediction Model of the CFM56-5B Turbofan Engine". In: (2017), pp. 1–118 (cit. on p. 22).

[18] 3. Systems. *How does Best Fit Alignment determine how the parts are aligned?* URL: https://support.3dsystems.com/ (cit. on p. 25).

[19] C. C. T. Center. *LOW PRESSURE TURBINE STAGE 1 NOZZLE SEGMENTS - INSPECTION*. First edition. CFM International, 2022 (cit. on p. 26).

[20] A. Gameros. "State-of-the-art in fixture systems for the manufacture and assembly of rigid components: A review". In: (2017), pp. 1–118 (cit. on pp. 31, 32).

[21] E. K. Henrikesn. *Jig and Fixture Design Manual*. Second edition. Academy of Technical Sciences, 1973 (cit. on p. 39).

[22] Norelem. *Posicionadores com mola fenda e esfera, em aço, com trava LONG-LOK*. URL: https://www.norelem.com/pt/pt/Produtos/Vis%C3%A3o-geral-de-produtos/Sistema-flex%C3%ADvel-de-pe%C3%A7as-normalizadas/03000-Posicionadores-com-mola-Pinos-de-reten%C3%A7%C3%A3o-Batentes-Elementos-de-centraliza%C3%A7%C3%A3o-e-posicionamento-Fixa%C3%A7%C3%B5es-Porcas-T/Posicionadores-com-mola/03001-Posicionadores-com-mola-fenda-e-esfera-em-a%C3%A7o-com-trava-LONG-LOK.html (cit. on pp. 42, 43).

[23] renishaw. *RSP3 REVO scanning probe*. URL: https://www.renishaw.com/cmmsupport/knowledgebase/en/rsp3--22119 (cit. on pp. 43–45).

[24] E. ToolBox. *Friction Coefficients and Calculator*. URL: https://www.engineeringtoolbox.com/friction-coefficients-d_778.html (cit. on p. 46).

[25] Mitutoyo. *CAT1000PS - User Manual*. Mitutoyo, 2019 (cit. on p. 61).

A

Appendix

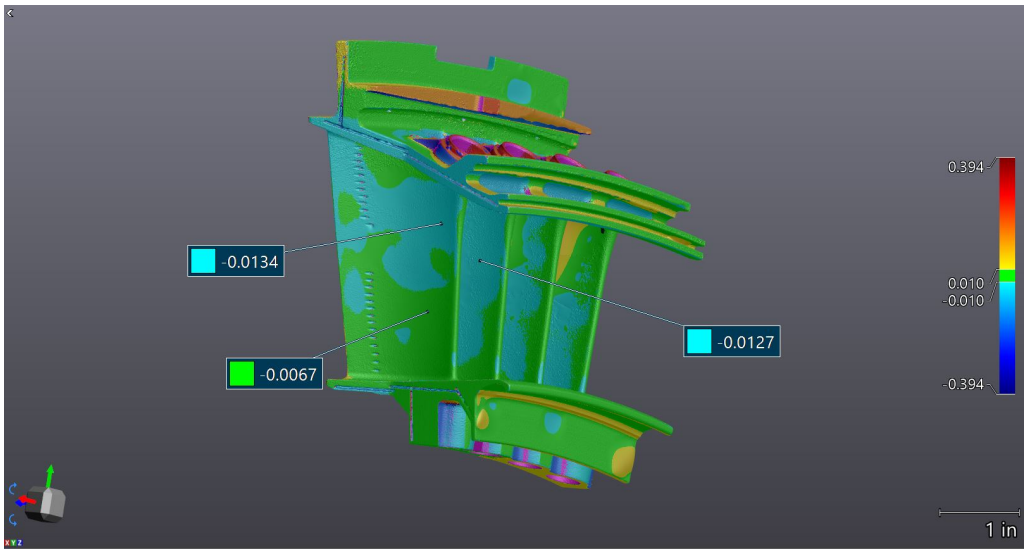

Figure A.1: Front view of body compare.

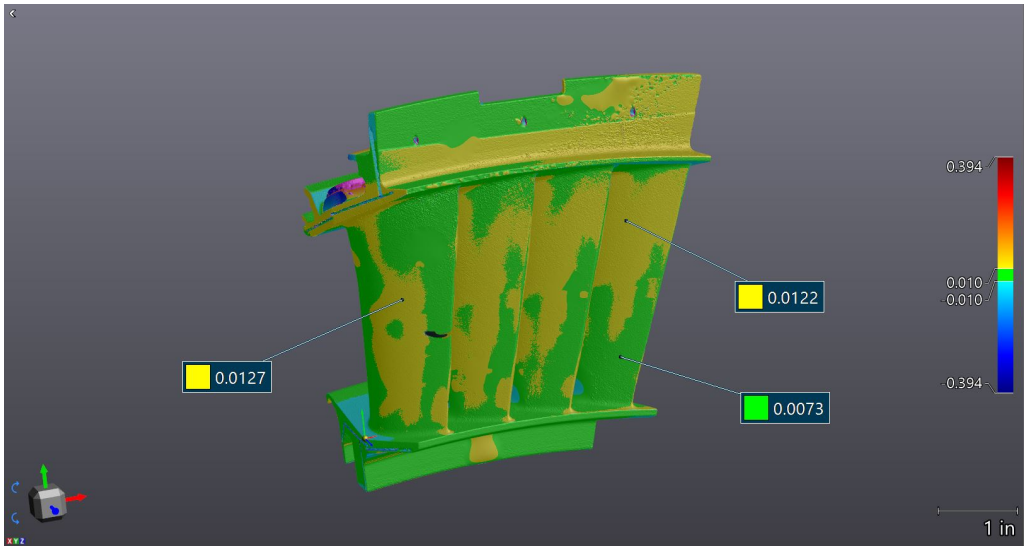

Figure A.2: Back view of body compare.

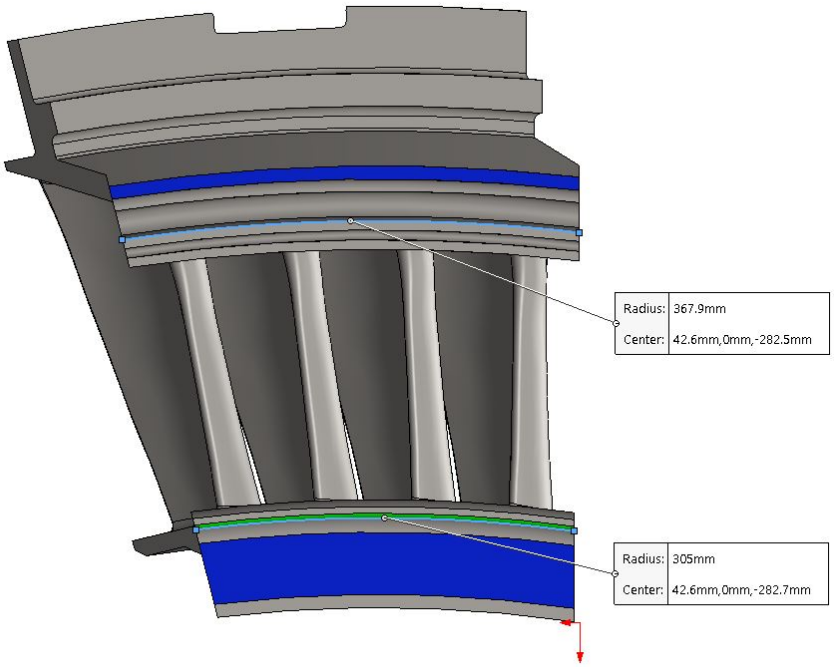

Figure A.3: Guided surface's radius curvature.

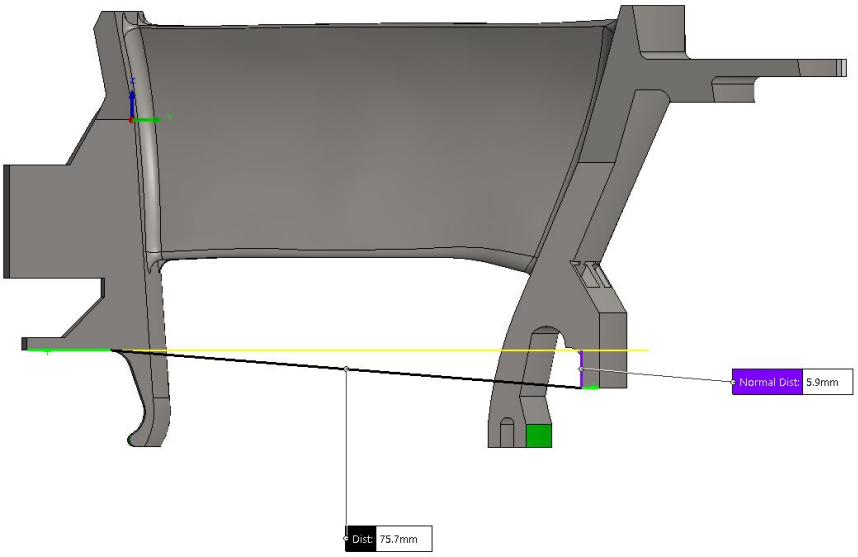

Figure A.4: Vertical distance between seating surfaces.

No.		Function	Parameters
1 1		Change probe tree	No. of probe tree = 3
2 2		Change probe	1
3 3		CNC on/off	On
4 4		Load co-ord. system	82
5 5		Set relation to CAD co-ord. system	Defined; apply future co-ordinate system chang
6 6		Load co-ord. system	82
7 7		Clearance height	Clearance height on Z axis = 1.1811
8 8		Load co-ord. system	82
9 9		Clearance height	Clearance height on Z axis = 1.1811
10 10		CNC on/off	On
11 11		Move Absolute movement	X = 6.9809 Y = 1.8016 Z = 24.0090
12 12		Subprogram	BF106 Library = No
13 191		Set relation to CAD co-ord. system	Defined; apply future co-ordinate system chang
14 192		Move Absolute movement	X = 5.0740 Y = 0.0285 Z = 7.0997
15 193		Change probe	14
16 194		Clearance height	Clearance height on Z axis = 1.1811
17 195		Contour	Section 11 (1) Mean
20 199		Connection element Contour	A20 (2)
21 203		Min. max. of contour Point	A20 (2) point (7); Last point of contour
22		Min. max. of contour	A20 (2)
26 215		Align base plane	SURF (1) XY plane, Origin in element
27 216		Clearance height	Clearance height on Z axis = 1.1811
28 218		Connection element Contour	A20 Align (3)
29 222		Contour Store contour	A20 Align (3) C:\Users\EAC\Desktop\MEASURED_last2.G\
30 223		Load variables from file	C:\MCOSMOS\TEMP\CtEval.res
31 224		Formula calculation	Area = CntrArea
32 225		Contour Export contour	A20 Align (3) E:\A20\A20 2D inch.igs
33 226		Contour Export contour	A20 Align (3) E:\A20\A20 2D mm.igs
34 227		Contour Export contour	A20 Align (3) E:\A20\A20 3D mm.igs
35 228		Contour Export contour	A20 Align (3) E:\A20\A20 3D inch.igs

Figure A.5: CMM program commands.

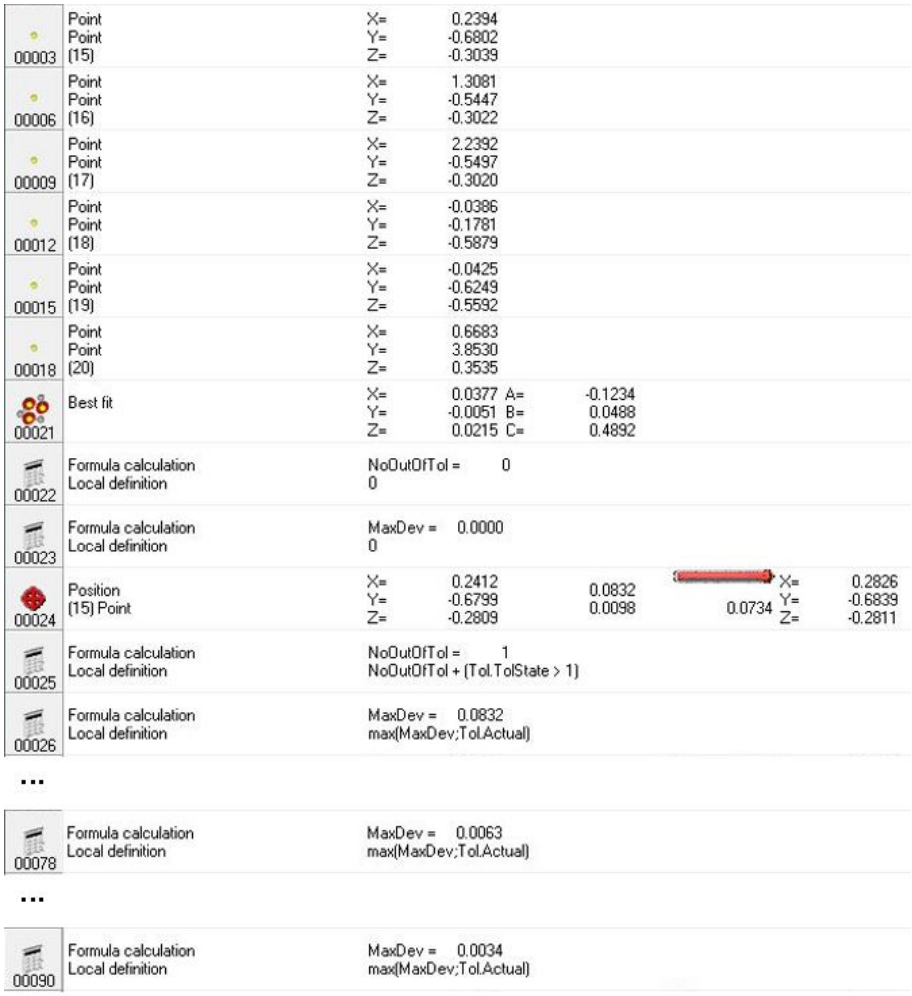

Figure A.6: Best-fit alignment commands.

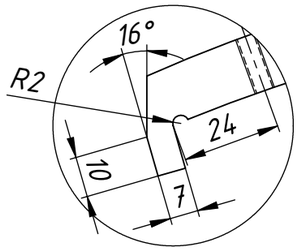

DETAIL C
SCALE 2 : 3

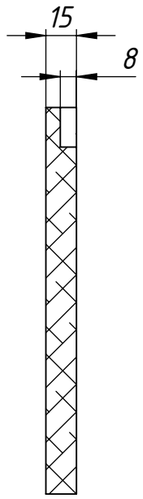

SECTION B-B

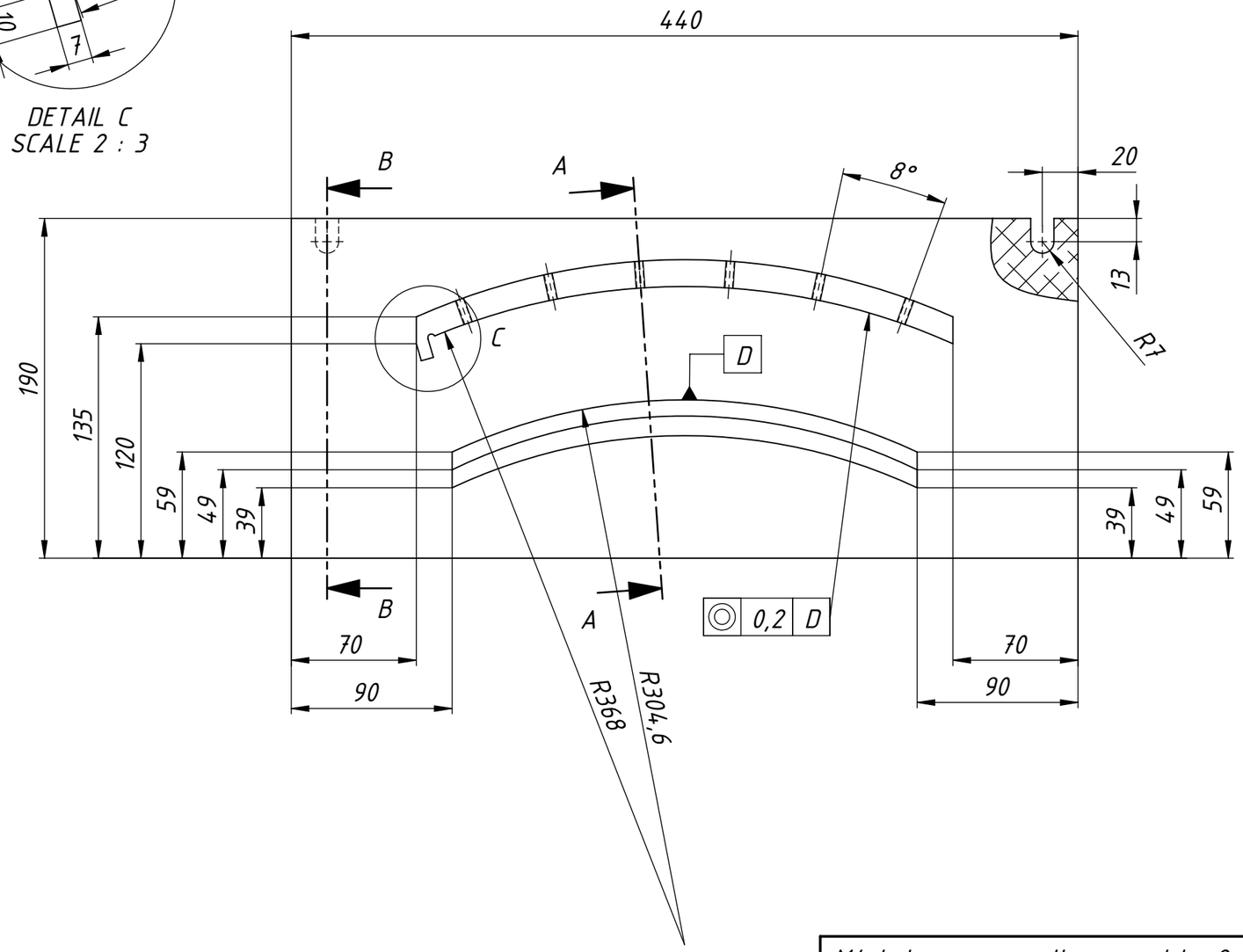

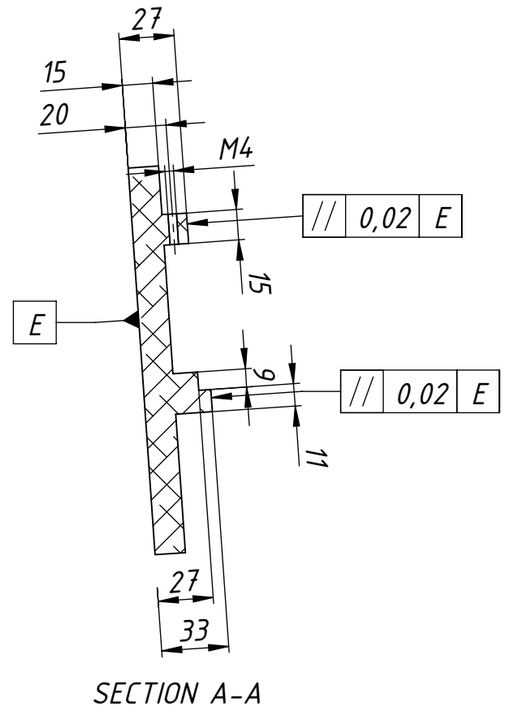

SECTION A-A

M4 holes are equally spaced by 8 degrees.

Designed	6/8/22		FCT-UNL TAP M&E	António Guerreiro 53122
Drawn	6/8/22			
Copy	6/8/22			
Verif.				
Scale 1:3			Fixture Tool	PTPMM53122

I

Annex 1

ZEISS Calypso

Plano de prueba
PRELIM_DBP1 CFM56-7B_v1

Fecha
22 Agosto 2022

N° SO
22221604

Número de plano
338-108-

Hora
9:35:28

Pedido
INITIAL GASPATH

Inspector
793

MMC
C32Bit

Número pieza
DB788671

Duración med.
00:04:56,0

	Valor real	Valor nom.	Tol. sup.	Tol. inf.	Desviación
	Section passage -1 ssc				
	885.932	838.980			46.952
	Section passage 1 ssc				1.849
	855.999	838.980	15.170	-25.170	17.019
	Section passage 2 ssc				
	852.571	838.980	15.170	-25.170	13.591
	Section passage 3 ssc				
	852.422	838.980	15.170	-25.170	13.442
	Section passage 4 ssc				
	813.961	838.980			-25.019
	Section passage -1 et 4				10.023
	864.173	838.980	15.170	-25.170	25.193
	Section totale ssc				40.939
	3410.939	3355.920	14.080	-50.350	55.019

Figure I.1: Throat area report for reference nozzle.

ZEISS Calypso

ZEISS

Plano de prueba DBP1 CFM56-7B_sans_scanning_v2	Fecha 2 Junio 2022	N° SO 22178049
Número de plano 338-108-	Hora 16:04:06	Pedido GASPATH TEST
Inspector 689	MMC C32Bit	Número pieza BA26917A
		Duración med. 00:06:25,0

	Valor real	Valor nom.	Tol. sup.	Tol. inf.	Desviación
	Section passage -1 ssc 856.097	838.980			17.117
	Section passage 1 ssc 865.053	838.980	25.170	-25.170	0.903 26.073
	Section passage 2 ssc 842.990	838.980	25.170	-25.170	|- 4.010
	Section passage 3 ssc 833.899	838.980	25.170	-25.170	-| -5.081
	Section passage 4 ssc 791.693	838.980			-47.287
	Section passage -1 et 4 812.070	838.980	25.170	-25.170	-1.740 -26.910
	Section totale ssc 3365.836	3355.920	50.320	-50.350	|- 9.916

Figure I.2: Throat area report for secondary nozzle.